UNIVERSIDADE DA BEIRA INTERIOR
Engenharia

Internal Ballistics Simulation of a Solid Propellant Rocket Motor

Marc Faria Gomes

Dissertação para obtenção do Grau de Mestre em
Engenharia Aeronáutica
(Ciclo de estudos integrado)

Orientador: Prof. Doutor Francisco Brójo

Covilhã, Outubro de 2013

Resumo

Na concepção e desenvolvimento de motores foguete sólidos, o uso de ferramentas numéricas capazes de simular, prever e reconstruir o comportamento de um dado do motor em todas as condições operativas é particularmente importante, a fim de diminuir todos os custos e planeamento.

Este estudo é dedicado a apresentar uma abordagem para a simulação numérica de balística interna de um determinado motor foguete de propelente sólido, Naval Air Warfare Center no. 13, durante a fase quasi steady state por meio de uma ferramenta numérica comercial, ANSYS FLUENT.

O modelo de balística interna construído neste estudo é um modelo axissimétrico 2-D. Tem por base vários pressupostos. Entre eles, está o pressuposto de que não há contribuição da queima erosiva e da queima dinâmica no modelo da taxa de queima.

Os resultados da simulação balística interna são comparados com os resultados encontrados na pesquisa bibliográfica, validando assim, o modelo que foi construído. A validação dos resultados também nos permite concluir que os pressupostos assumidos na construção do modelo são razoáveis.

Sugestões e recomendações para um estudo mais aprofundado são delineadas.

Palavras-chave:
Simlulação de balística interna; motor foguete de propelente sólido; ANSYS FLUENT; NAWC no. 13.

Acknowledgments

There is only one person coming to mind while I am writing this section. Dr Francisco Brójo, thank you for your help, guidance, support, dedication, patience and motivation throughout this project but also for your inspiring teaching during the taught part of the course.

Abstract

In the design and development of solid propellant rocket motors, the use of numerical tools able to simulate, predict and reconstruct the behaviour of a given motor in all its operative conditions is particularly important in order to decrease all the planning and costs.

This study is devoted to present an approach to the numerical simulation of a given SPRM internal ballistics, NAWC no. 13, during the quasi steady state by means of a commercial numerical tool, ANSYS FLUENT.

The internal ballistics model constructed in this study is a 2-D axisymmetric model, based on several assumptions. Among them is the assumption that there is no contribution of the erosive burning and the dynamic burning in the burning rate model.

The results of the internal ballistics simulation are compared with the results found in the bibliographical research, thus validating the model that has been set up. The validation of the results also allows us to conclude that the assumptions made in the construction of the model are reasonable.

Suggestions and recommendations for further study are outlined.

Keywords:
Internal ballistics simulation; Solid propellant rocket motor; ANSYS FLUENT; NAWC no. 13.

Contents

List of Figures

List of Tables

List of Symbols

Acronyms

AN	Ammonium Nitrate
AP	Ammonium Perchlorate
BLT	Boundary Layer Transition
CEA	Chemical Equilibrium with Applications
CFD	Computacional Fluid Dynamics
CMDB	Composite-Modified Double-Base
GPS	Global Positioning System
GREG	Grain REGression model
HMX	Cyclotetramethylene tetranitramine
HTPB	Hydroxyl-Terminated PolyButadiene
IT	Ignition Transient
LPRM	Liquid Propellant Rocket Motor
MEOP	Maximum Expected Operating Pressure
MUG	Multidimensional Unsteady Gasdynamics
NAWC	Naval Air Warfare Center
NG	Nitroglycerine
N-M	Non-military
PB	Polybutadiene
PBAN	Polybutadiene-acrylic acid-acrylonitrile terpolymer
PU	Polyurethane
Q1D	Quasi 1D
QSS	Quasi Steady State
RDX	Cyclotrimethylenetrinitramine
RNG	Renormalization Group Theory
SPINBALL	Solid Propellant rocket motor Internal Ballistics
SPIT	Solid Propellant rocket motor Ignition Transient
SPP	Solid propellant rocket motor Performance Program
SPRM	Solid Propellant Rocket Motor
SRAM	Short-Range Attack Missile
TO	Tail Off

Nomenclature

A	Area
a	burn rate coefficient
C	Effective exhaust velocity
C_F	Thrust Coefficient
c_p	specific heat
c^*	Characteristic velocity
D	Diameter
F	Thrust
g_0	Standard acceleration of gravity
I_{sp}	Specific impulse
I_t	Total impulse
$\mathfrak{M}$	molecular weight
m	mass
$\dot{m}$	mass flow rate
n	burning rate exponent
p	pressure
q	heat flux
R	Universal gas constant
r_b	burning rate
T	Thrust
t	time
u	exhaust velocity

Greek symbols

γ	ratio of specific heats
ε	nozzle expansion ratio
ρ	density

Sub- and Superscripts

a	ambient
b	propellant
c	chamber
e	exhaust
n	burnrate exponent
0	nominal value
*	throat

Chapter 1

Introduction

In this introductory chapter a brief description of the thesis is presented with the intent of this study, motivation and objectives. It considers the framework of the work and its importance. Finally, a brief overview of the structure of the dissertation is shown.

1.1 Motivation

To be an engineer it is mandatory that I present a research in my final year of university, a dissertation, to acquire my master sheet degree. Many possibilities of research were presented. However, I have chosen the presented subject not only to fully examine the type of technology in question, learning the physical principles and consequently mathematical fundamental equations on how the rocket works and an appreciation of all the applications of rocket propulsion, but also to understand how the space exploration, that gives and will continue to give so much answers to mankind, was made possible, how it will increase and reach answers beyond common expectations.

1.2 Objectives

This study is devoted to present an internal ballistics model for a solid propellant rocket motor during the entire combustion of the propellant, i.e., to design and develop a solid propellant rocket motor using a numerical tool, ANSYS FLUENT, which creates the possibility to simulate and predict the behaviour of the given motor in its operative conditions.

1.3 Framework

In order to fully understand the importance of the invention of the rocket and therefore the importance of this study, we need to understand that the human development, and consequently the civilisation development, is unquestionably linked with transportation, war and commerce. It is irrefutable that the domestication of the horse and the invention of the wheel had a dramatic effect on civilisation. But, without entering too much in the history of the rocket, it is essential that we see the connection between the rocket and mankind.

In the last millennium, rockets were used in wars, since 1275 by Kublai Kahn. In the fields of transportation and communication, the soviet union space program achieved great results, in the period from 1957 to 1959. They successfully launched three satellites, the first one was Sputnik in 1957, and two lunar probes and in 1961 Yuri Gagarin became the first man in space. Among these achievements the USSR space program was also effectively able to launch the first spacecraft to the Moon, the first docking of two spacecraft and the first space station.

So now, in this new millennium, the rocket is seen as the emerging revolution in transport. It is true that so far, only a few humans have actually travelled in rocket-propelled vehicles, but an astonishing amount of commercial and domestic communication is now reliant on satellites, where rocket propulsion is the essential transportation technology for this rapid growth in human communication and exploration. Also, the proposed return to the Moon and the new plans to send humans to Mars reveal a resurgence interest in space exploration which cannot be achieved without rocket propulsion. Rockets are the key to space exploration, space science and space commerce.

To conclude, from its beginnings in ancient China, through its development during the wars as a weapon, during the cold war as a weapon and transportation technology, rocket propulsion has become the essential technology.

1.4 Structure of the Work

The present Master thesis is organized, excluding the introductory chapter, as following:

- Chapter 2: Rocket motors. It presents which types of rocket motors exist and describes the solid propellant rocket motors (SPRM) concept necessary to explain the internal ballistic rocket.

- Chapter 3: This chapter deals with the existing models of internal ballistics, defining the necessary parameters for its calculation.

- Chapter 4: Describes the simulation of internal ballistics, defining the construction of the model. It shows the results of the simulation, validated by

comparison with other works results.

- Chapter 5: In this final chapter, not only the final conclusions are presented but also suggestions for future research.

Chapter 2

State of the Art

In this chapter, the principles of rocket propulsion are presented along with a classification of the types of rocket, with particular and detailed attention to the solid propellant rocket motor, focusing on important definitions, principles and processes related with internal ballistics.

2.1 Rocket Motors Classification

Rockets are generally classified as either "chemical" or "non chemical", depending upon whether the energy that appears in the propellant streams arises from the release of internal chemical energy via a chemical reaction or is supplied to the propellant from an external source.[25]

2.1.1 Chemical Rockets

The "chemical" rocket or "thermal" rocket is a heat engine, i.e., it converts the heat, generated by the combustion of the propellants, into kinetic energy of the emerging exhaust gas. The momentum carried away by the exhaust gas provides the thrust, which accelerates the rocket. "Chemical" rockets are further subdivided in solid propellant rocket motors, liquid propellant motors rockets, hybrid propellant rocket motors and gel rocket motors.

- Solid propellant rocket motors

  This thesis is focused only on this type of rocket, so a full detailed explanation based on SPRMs will be presented at 2.2.

- Liquid propellant rocket motors

  To date, the most frequently utilized rocket in large boosters has been liquid propellant rocket motors (LPRM) [25].

A LPRM consists of one or more combustion or thrust chambers into which both fuel and oxidant, stored into one or more propellant tanks, are pumped by a feed mechanism. It also consists of a power source to furnish the energy for the feed mechanism, suitable plumbing or piping to transfer the liquids, a structure to transmit the thrust force and control devices to initiate and regulate the propellant flow and hence the thrust, and an expansion nozzle which converts the high-pressure hot gas, generated by the combustion, into a high velocity exhaust stream. It is the expansion of the hot gas against the walls of the nozzle that does the work and accelerates the rocket.

In the simplest system, the propellant is fed to the combustion chamber by static pressure in the tanks. High-pressure gas is introduced to the tank, or is promoted evaporation of the propellant forcing the fuel and oxidiser into the combustion chamber. A typical turbopump-fed LPRM system is shown in figure 2.1.

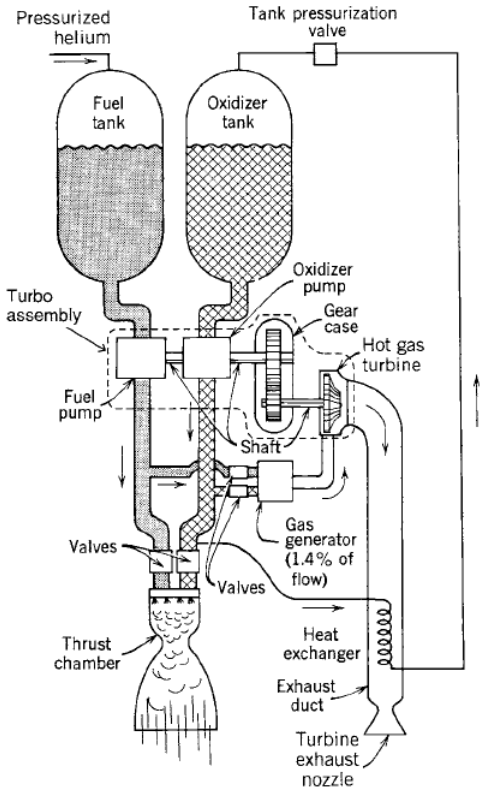

Figure 2.1: Typical turbopump-fed liquid propellant rocket engine.[28]

The LPRM can be divided in two categories, those used for boosting a payload and imparting a significant velocity increase to a payload, and those

used in auxiliary propulsion for trajectory adjustments and attitude control. Beyond that, they can also be classified according to their use, i.e., if their are "reusable" or suitable for a single flight only, and "restartable" or "single firing". Nevertheless, they can also be categorised by their propellants, application, thrust level and feed system type (pressurised or turboprop).

The main advantage of the LPRM is that it can be randomly throttled, stopped and restarted. Many propellants have non-toxic exhaust and the emission of plume radiation and smoke are usually low.

The disadvantages of the LPRM, as compared to the SPRM, are that they have more complex designs with more parts or components, thus it is expectable a lower reliability for this type of rockets than for the SPRM. . They require more volume because of the lower average propellant density and the packaging of engine components. Some propellants produce toxic vapors. Besides, a persistent problem encountered in the LPRM is that of instabilities, like "chugging", "buzzing" and "screaming".[21, 25]

- Hybrid propellant rocket motors

  While, as we will see, the SPRM contains both fuel and oxidant in the charge or grain, the hybrid motor only has the fuel in the charge, the oxidant is introduced as a liquid propellant, injected and atomised just like in the case of a LPRM.

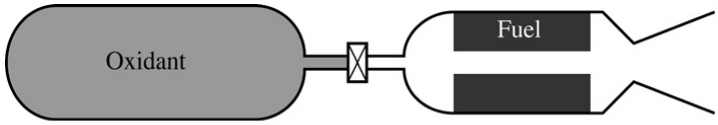

Figure 2.2: Schematic of a hybrid rocket motor.[31]

This type of rocket was first largely researched but later on was neglected, except for some small number of specialised applications. More recently, it has come to prominence for two specific applications. Amateur rockets, where its builders find the safety and simplicity of the hybrid rocket attractive, and there are commercially rockets available for this purpose. However, there are also applications suitable for human spaceflight.

The hybrid rocket requires two steps to burn: first, the solid fuel must be heated and vaporised and then mixed with the introduced oxidant. Therefore, the possibility of an accident decreases. Indeed, accidental contact between cold fuel and oxidiser has no effect because they are in different material states. Another advantage of the hybrid rocket is that it can be shut down, just like a LPRM can, simply by closing the valve supplying the liquid oxidant.

The basic configuration of the hybrid thrust chamber is largely the same as for a SPRM, as we will see. The fuel is cast in the casing and there is a nozzle to develop the thrust from the hot gas generated. The grain is cast into the casing, with no parts of the casing wall accessible to the hot gas. The areas not protected by the fuel grain have to be covered with ablative coolant material. The design of the casing has to take into account the pressure developed during firing and the requirement to optimise mass-ratio by keeping the dry mass of the motor low. In this regard, the hybrid rocket and SPRM have identical requirements, although the grain cross-section and the specific details of the thrust chamber are different and display a fundamental difference in the operation when compared to the SPRM.

Hybrid rockets have a role to play in space propulsion, where their relative safety and simplicity show advantages. The development process is to increase the thrust so that they can be used for large human launchers. However, this process is by no means complete at the present.[31]

- Gaseous propellant rocket motor

  Gaseous propellant rocket motors use a stored high pressure gas as their working fluid or propellant. They are similar to the liquid propellant rocket motors, since the stored gas requires relatively larger and heavier tanks and require complex feed mechanisms. Gaseous propellant rocket motors are the least used type of rocket motors.[4, 14]

- Gel propellant rocket motor

  Generally, gels are liquids whose properties have been modified by the addition of gelling agents, which results in a behaviour that resembles that of solids.

  The need for the development of gel propellants arises from the significantly higher energetic performance of metallized fuels in bi-propellant systems in comparison to non-metallized, hydrocarbon fuels. The properties of gels allow the addition of metal particles that can be suspended within the fuel matrix, enhancing both the energy and the energy density of the motor.

  Gelled propellant propulsion systems have significantly reduced "personnel-hazard risks from inadvertent handling errors or unplanned events when compared with neat liquid or solid propellant systems due to the gel propellants" unique, thixotropic fluid behaviour, i.e., the fluid is able to form a gelled structure over time when it is not subjected to shearing and to liquefy when agitated.

  Gel propellants can be defined as propellants that during storage behave as viscoelastic solids. During the feeding process their viscosity decreases under

shear stress to the degree of liquefaction and finally are atomized and burn as liquids.

One of the most significant advantages of the gelled propellant is that the gel surface hardens in contact with a gaseous environment, thus, in case of feeding system failure during storage, the leakage rate is reduced, compared to liquids. The volatility of gels is lower than that of liquids propellants and in case of leak or spill, much less vapours will be released, reducing toxicity hazards. Additionally, long-term storage without settling or separation is possible and as far as the environmental issues are concerned, many spilled gelled propellants can be diluted with water and disposed of safely. Finally, energy management capability similar to liquids is possible for gelled propellants.

However, there is a small decrease in specific impulse due to dilution with a gelling agent and less efficient atomization or combustion. The propellant loading or unloading propellant procedures are more complex. The changes in ambient pressure cause changes in propellant density and viscosity, which can result in more residual propellant, hence a reduction of available total impulse. Finally, the price of a gel propellant is around 30% higher than the price of a solid propellant.[17, 21]

2.1.2 Non Chemical Rockets

There is an elegant simplicity in the process of generation of thrust by the chemical rockets, however, when "very-high-energy" missions are intended, there is a fundamental limitation, no more energy can be put into the rocket than is contained in the propellant supplied to the motor. Thus, even with the use of the most energetic of chemical propellants, the required fraction of propellant mass to overall vehicle mass becomes excessive.

Although the arrival of the space age was possible by using the chemical rocket technology, by stretching its ability to the limit through multi-staging, and on motors that perform very close to their theoretical best, and even if more ambitious space programs, like going to Mars could be achieved, but would require a very large effective mass ratio and all the propellant require would need to be raised to Earth orbit, it would be obviously preferable if more propulsive power could be extracted from the propellant and the exhaust velocity could be increased.[25]

- Nuclear rocket

  A conceptually simple idea that dates back almost to the begging of the twentieth century, the nuclear rocket operates by having the propellant pass through heat-exchange passages within a nuclear reactor and then through a propelling nozzle. Three different types of nuclear energy sources have been researched for delivering heat to a working fluid, usually liquid hydrogen (see

figure 2.3), which subsequently can be expanded in the nozzle and thus accelerated to high ejection velocities (6000 to 10000 m/s), almost twice of the best chemical rockets.

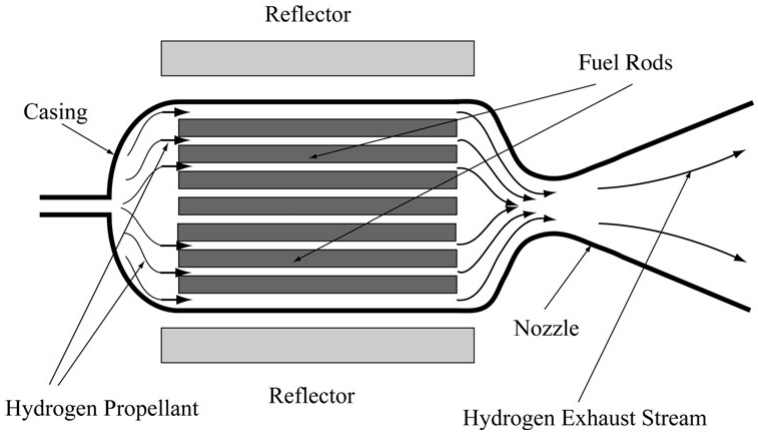

Figure 2.3: The principle of nuclear propulsion.[31]

They are the fission reactor, the radioactive isotope decay source and the fusion reactor, basically they all are an extent of LPRM. The advantage of a nuclear rocket appears because of the freedom in the choice of propellants. The most desirable propellant for such a system is the one that gives the maximum possible specific enthalpy for the giving limiting temperature. The specific enthalpy of a perfect gas is approximately inversely proportional to the molecular weight, which is the reason that the most common propellant for the nuclear rocket is liquid hydrogen.
Even if the related mass ratio for a very-high-energy mission could be less than one third than the one for a chemical rocket, the nuclear rocket gives an insufficient exhaust velocity for use in manned planetary missions. But if these problems were to be fixed, there would still be limitations to nuclear rockets, due to the "Outer Space Treaty" of 1967, where was agreed that nuclear weapons are banned in orbit around Earth, and probably the same will happen even to "nuclear tugboats".[31, 25]

- Electrical rocket

  Although the concept of electric propulsion has been known for quite a long time and different types of electric thruster have been developed and tested in space, they have remained a curiosity due to their heavy and inefficient power sources. However, in recent years, it was realised that the requirement for high velocity did not apply only to ambitious space programs but also to

station keeping for communications satellites, and a revived interest emerged in electrical propulsion.

In all electric propulsion, the source of the electric power (solar radiation receivers or batteries) is physically separated from the mechanism that produces the thrust. Three types have been developed, the electrothermal rocket propulsion, which most resembles the chemical rocket, the propellant is heated electrically by heated resistors or electric arcs (figure 2.4) and the hot gas is then thermodynamically expanded and accelerated though an exhaust nozzle. The other two types, the electrostatic or ion propulsion rocket and the electromagnetic or magnetoplasma rocket, achieve propulsion by different principles. Nevertheless, both of them only work in vacuum, and the thermodynamic expansion of a gas in the nozzle, does not apply.

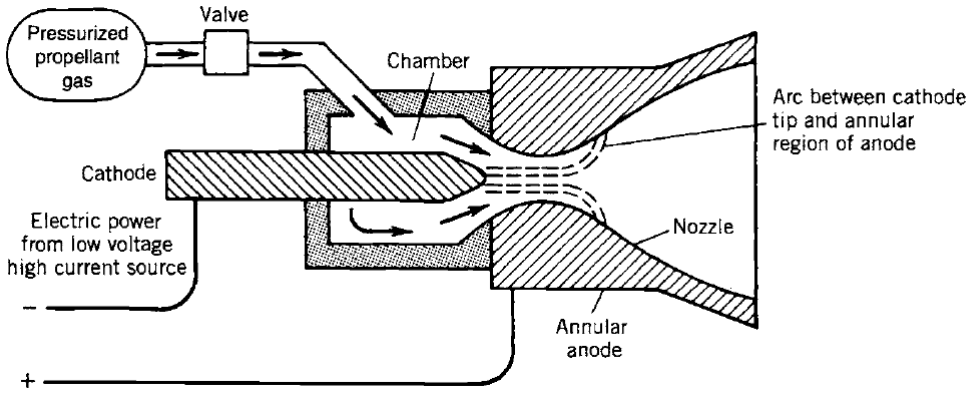

Figure 2.4: Simplified schematic diagram of arc-heating electric rocket propulsion system.[28]

For an ion rocket (figure 2.5) the working fluid, typically xenon, is ionized and then the electrically charged heavy ions are accelerated to very high velocities (2000 to 60000 m/s) by means of electrostatic fields. The ions are subsequently neutralized, i.e., combined with electrons to prevent charged particles on the vehicle.

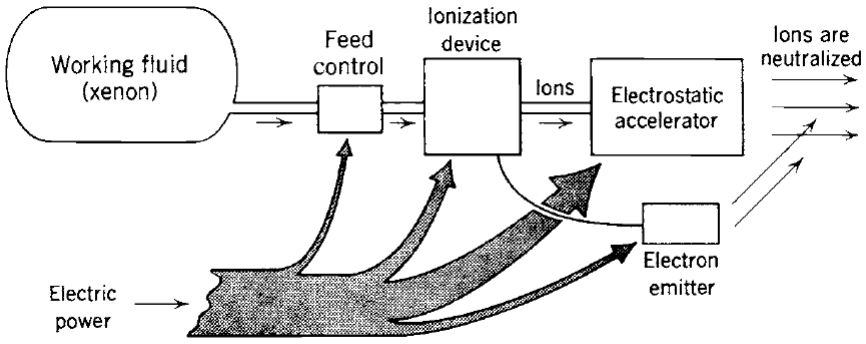

Figure 2.5: Simplified schematic diagram of a typical ion rocket.[28]

In the magnetoplasma rocket, an electrical plasma, i.e., an energized hot gas containing ions, electrons and neutral particles, is accelerated by the interaction between electrical currents and magnetic fields and ejected at high velocity (1000 to 50000 m/s). There are many types and geometries. A simple pulsed unit with a solid propellant is shown in figure 2.6.

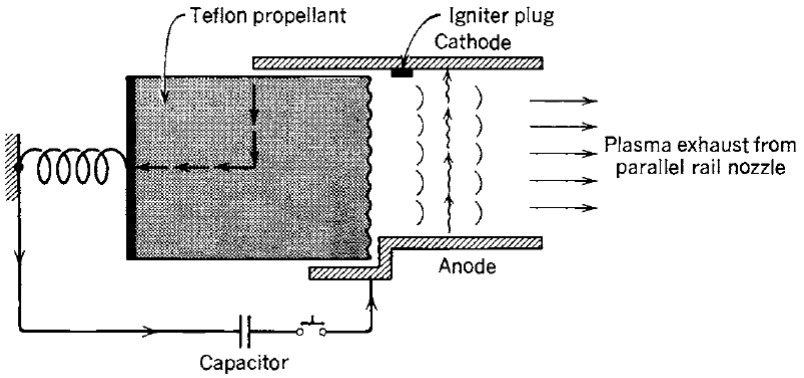

[28]

Figure 2.6: Simplified diagram of a rail accelerator for self-induced magnetic acceleration of a current-carrying plasma.

Several technologies exist for harnessing solar energy to provide the power for spacecraft and also to propel spacecraft using electrical propulsion. An attractive concept, the solar thermal rocket, figure 2.7, has large diameter optics to concentrate the sun's radiation, e.g., by lightweight precise parabolic mirrors or Fresnel lenses onto a receiver or optical cavity.

However, the concept has problems being investigated, including, lightweight

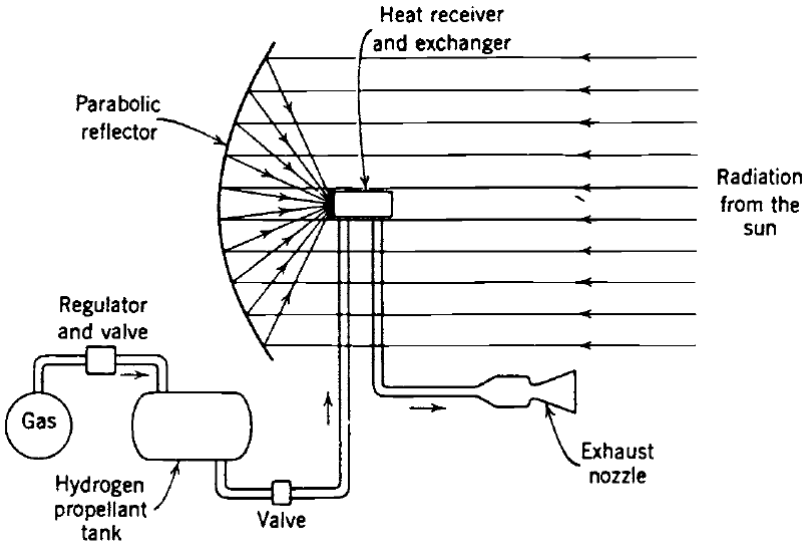

Figure 2.7: Simplified schematic diagram of a solar thermal rocket concept.[28]

mirror or lens structures, operational life, minimizing hydrogen operation and heat losses to other spacecraft components. To date, the solar thermal rocket has not yet been the principal thrust of flying spacecraft.[31, 25]

2.2 Solid Propellant Rocket Motors

Considering the complexities of the liquid propellant rocket engine, it does not seem remarkable that so much attention has been given to the design and development of the much simpler solid propellant motor.[31]

2.2.1 Basic Configuration

A SPRM (figure 2.8), operates, thermodynamically, in the same way of a LPRM. The hot gas produced by the combustion is converted to a high speed exhaust stream in exactly the same way and so the nozzle, the throat and the restriction in the combustion chamber leading to the throat are all identical in form and function. The difference lays in the propellant form, the fuel and the oxidant are pre-mixed in solid form and are contained within the combustion chamber.

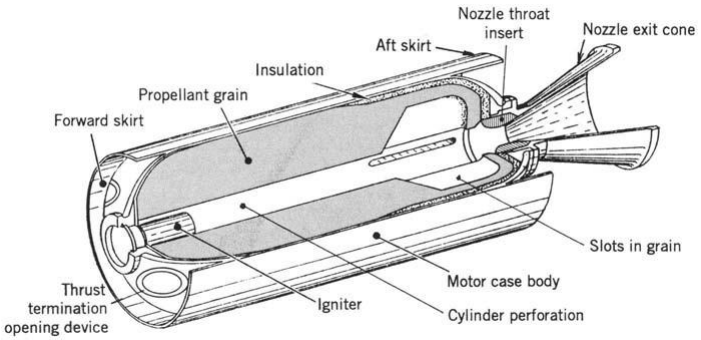

Figure 2.8: Typical SPRM with the propellant grain bonded to the case and the insulation layer and with a conical exhaust nozzle.[28]

The hot gas is produced by combustion on the hollow surface of the solid fuel block, known as the charge or grain. In the majority of cases the grain is bonded to the wall of the combustion chamber to prevent access of the hot combustion gases to any surface of the grain not intended to burn and to prevent heat damage to the combustion chamber walls. The grain contains both fuel and oxidant in a finely divided powder form, mixed together and held by a binder material.

The combustion chamber of a SPRM is very simple, in comparison to a LPRM. It consists of a casing for the propellant, which joins to a nozzle of identical geometry to that of a LPRM. Once the inner surface of the grain is ignited, the motor produces thrust continuously until the propellant is exhausted.[31]

2.2.2 The Properties and the Design of Solid Motors

As it was said before, in comparison with a LPRM, the SPRM is very simple, and the design issues are therefore fewer. There is no injector and no propellant distribution system. Design issues related to the propellant are mostly concerned with the selection of the propellant type and the mounting and protection of the propellant in the casing. There are no propellant tanks, however the casing has to contain the propellant and also behave as a combustion chamber. For boosters the casing is large, and to combine large size with resistance to high combustion pressure is very different from the same issue in a liquid system where the requirements are separated. Cooling is completely different because there are no liquids involved and heat dissipation has to be entirely passive.

To obtain thrust stability in a SPRM is very complicated, the supply of combustible material is dependent on conditions in the combustion chamber and there are increased chances for instabilities to arise and propagate. Associated with stability is thrust control and for a SPRM the thrust depends on the rate of supply of combustible propellant, this depends on the pressure and temperature at the burning surface and it cannot actively be controlled. As mentioned before the mo-

tor produces thrust continuously until the propellant is exhausted. These design issues are central to the correct performance of a SPRM.

While the SPRM is essentially a single-use item, the cost of large boosters is very high and the necessary engineering quality of some of its components, specially the casing may make them suitable for reuse. This was a design feature for both the Space shuttle, where boosters are recovered and the segments reused, and the Ariane 5 solid boosters, where the boosters are recovered for post-flight inspection only.[31, 28]

2.2.3 Solid Propellant

The choice of propellant is relatively narrow for a SPRM and critical to the rocket motor design. The desirable propellant characteristics are listed below:

1. High gas temperature or high specific impulse, i.e., high gas temperature and/or low molecular mass;
2. Predictable, reproducible and initially adjustable burning rate to fit the need of grain design and the thrust-time requirement;
3. For minimum variation in thrust or chamber pressure, the pressure or burning rate exponent and the temperature coefficient should be small;
4. Adequate physical properties, including bond strength, over the intended operating temperature range;
5. High density, thus allowing a small-volume motor;
6. Predictable, reproducible ignition qualities;
7. Good ageing characteristics and long life, which predictions depend on the propellant's chemical and physical properties;
8. Low absorption of moisture, which often causes chemical deterioration;
9. Simple, reproducible, safe, low-cost controllable and low-hazard manufacturing;
10. Guaranteed availability of all raw materials and purchased components over the production and operating life of the propellant and good control over undesirable impurities;
11. Low technical risk, such as a favourable history of prior applications;
12. Relative insensitivity to certain energy stimuli;
13. Non-toxic exhausts gas;

14. Not susceptible to combustion instability.

However, the requirements for any particular motor will influence the priorities of these characteristics which are occasionally in conflict with each other and some of these desirable characteristics will also apply to all materials and purchased components used in solid motors, such as igniters, insulator, case and arm device.

A variety of different chemical ingredients and propellant formulations have been synthesised, analysed and tested in experimental motors. The table 2.1 evaluates some of the advantages and disadvantages of several propellants classes.

Table 2.1: Characteristics of selected propellants.[28]

Propellant type	Advantages	Disadvantages
Double-base (extruded)	Modest cost; nontoxic clean exhaust, smokeless; good burn rate control; wide range of burn rates; simple well-known process; good mechanical properties; low temperature coefficient; very low pressure exponent; plateau burning is possible.	Free-standing grain requires structural support; low performance, low density; high to intermediate hazard in manufacture; can have storage problems with NG bleeding out; diameter limited by available extrusion presses.
Double-base (castable)	Wide range of burn rates; nontoxic smokeless exhaust; relatively safe to handle; simple, well-known process; modest cost; good mechanical properties; good burn rate control; low temperature coefficient; plateau burning can be achieved	NG may bleed out or migrate; high to intermediate manufacture hazard; low performance; low density; higher cost than extruded DB.
Composite-modified double-base or CMDB with some AP and Al	Higher performance; good mechanical properties; high density; less likely to have combustion stability problems; intermediate cost; good background experience.	Storage stability can be marginal; complex facilities; some smoke in exhaust; high flame temperature; moisture sensitive; moderately toxic exhaust; hazards in manufacture; modest ambient temperature range; the value of n is high (0,8 to 0,9); moderately high temperature coefficient.
Composite AP, Al, and PBAN or PU or CTPB binder	Reliable; high density; long experience background; modest cost; good aging; long cure time; good performance; usually stable combustion; low to medium cost; wide temperature range; high density; low to moderate temperature sensitivity; good burn rate control; usually good physical properties.	Modest ambient temperature range; high viscosity limits at maximum solid loading; high flame temperature; toxic, smoky exhaust; some are moisture sensitive; some burn-rate modifiers (e.g. aziridines) are carcinogens.
Composite AP, Al, and HTPB binder; most common composite propellant today	Slightly better solids loading % and performance than PBAN or CTPB; widest ambient temperature limits; good burn-rate control; usually stable combustion; medium cost; good storage stability; widest range of burn rates; good physical properties; good experience.	Complex facilities; moisture sensitive; fairly high flame temperature; toxic, smoky exhaust.
Modified composite AP, Al, PB binder plus some HMX or RDX	Higher performance; good burn-rate control; usually stable combustion; high density; moderate temperature sensitivity; can have good mechanical properties.	Expensive, complex facilities; hazardous processing; harder-to-control burn rate; high flame temperature; toxic, smoky exhaust; can be impact sensitive; high cost.
Composite with energetic binder and plasticizer such as NG, AP, HMX	Highest performance; high density; narrow range of burn rates.	Expensive; limited experience; impact sensitive; high pressure exponent.
Modified double-base with HMX	Higher performance; high density; stable combustion; narrow range of burn rates.	Same as CMDB above; limited experience; high cost.
Modified AN propellant with HMX or RDX added	Fair performance; relatively clean; smokeless; nontoxic exhaust.	Relatively little experience; can be hazardous to manufacture; need to stabilize AN to limit grain growth; low burn rates; impact sensitive; medium density.
Ammonium nitrate plus polymer binder (gas generator)	Clean exhaust; little smoke; essentially nontoxic exhaust; low temperature gas; usually stable combustion; modest cost; low pressure exponent.	Low performance; low density; need to stabilize AN to limit grain growth and avoid phase transformations; moisture sensitive; low burn rates.
RDX/HMX with polymer	Low smoke; nontoxic exhaust; lower combustion temperature.	Low performance; low density.

A typical propellant has between 4 and 12 ingredients. Representative formulations for three types of propellant are given in table 2.2 . In actual practice, rather than selecting a particular propellant for a particular purpose, each man-

ufacturer has its own precise and optimised propellant formulation, mixture and processing procedure. Also, the exact percentages of ingredients may differ not only among manufacturers but also between motor applications. The practice of adjusting the mass percentage and even adding or removing one or more of the minor ingredients is known as propellant tailoring, which is the technique of taking a well-know propellant and changing it slightly to fit a new application, different processing equipment, altered motor ballistics, storage life, temperature limits or even a change in ingredient source.[28]

Table 2.2: Representative propellant formulations.[28]

Double-Base (JPN) Propellant		Composite (PBAN Propellant)		Composite Double-Base (CMDB Propellant	
Ingredient	Wt %	Ingredient	Wt %	Ingredient	Wt %
Nitrocellulose	51,5	Ammonium perchlorate	70	Ammonium perchlorate	20,4
Nitroglycerine	43	Aluminum powder	16	Aluminum powder	21,1
Diethyl phthalate	3,2	Polybutadiene-acrylic acid-acrylonitrile	11,78	Nitrocellulose	21,9
Ethyl centralite	1	Epoxy curative	2,22	Nitroglycerine	29
Potassium sulfate	1,2			Triacetin	5,1
Carbon black	<1%			Stabilizers	2,5
Candelilla wax	<1%				

All common propellants can be manufactured, handled and fired safely, with proper precautions and equipment. Nonetheless, hazardous situations may arise, each material has its own set of hazards and not all apply to each propellant. The text below presents some of the more common hazards:

- Inadvertent ignition

  An inadvertent ignition can be caused by these effects:

  - Stray or induced currents activate the igniter;
  - Electrostatic discharge causes a spark or arc discharge;
  - Fires cause excessive heating of motor exterior, which can raise the propellant temperature above the ignition point;
  - Impact;
  - Energy absorption from prolonged mechanical mechanical vibration can cause the propellant to overheat.

  If a SPRM is ignited and starts combustion when it is not expected to do so, the consequences can include very hot gases, local fires or ignition of adjacent rocket motors. Unless the motor is constrained or fastened down, its thrust will suddenly accelerate it to unanticipated high velocities or erratic flight paths that can cause damage. Also, its exhaust cloud can be toxic and corrosive.

Usually an electromechanical system is provided that prevents stray currents from activating the igniter, arm system. It prevents electric currents from reaching the igniter circuit during its "unarmed" condition. When put into the "arm" position, it is ready to accept and transmit the start signal to the igniter.[1]

- Ageing and useful life

  The ageing of a propellant can be measured with test motors and propellant sample tests if the loading during the life of the motor can be correctly anticipated. It is then possible to estimate and predict the useful shelf or storage life of a rocket motor. Once this age limit or its predicted weakened condition is reached, the motor has a high probability of failure, so the old propellant needs to be removed and replaced to be considered safe to ignite and operate.[28, 1]

- Case overpressure and failure

  This type of motor failure can be caused by one the following phenomena:

  - The grain is over-aged, porous, or severely cracked and/or has major unbounded areas due to severe accumulated damage;
  - There has been a significant chemical change in the propellant due to migration or slow, low-order chemical reactions. This can reduce the allowable physical properties, weakening the grain, so that it will crack or cause unfavourable increases in the burning rate. In some cases chemical reactions create gaseous products which create small voids and raise the pressure in sealed stored motors;
  - The motor is not properly manufactured;
  - The motor has been damaged, e.g., a nick or a dent in the case caused by improper handling will reduce the case strength;
  - An obstruction plugs the nozzle and causes a rapid increase in chamber pressure;
  - Moisture absorption can degrade the strength and strain capabilities in propellants that contain hygroscopic ingredients.

  If any of these phenomena occurs, the chamber pressure will exceed the case's burst pressure and consequently the motor case will break or explode.[1]

- Detonation and deflagration

  A burning rocket motor propellant when burning over-pressurized can either deflagrate, i.e., burn, or detonate, explode violently. It can be possible for some propellants to change suddenly from an orderly deflagration to a detonation, thus the chemical reaction energy of the whole grain can be released

in microseconds. This transitions begins with with normal burning at rated chamber pressure, the hot gas then penetrates pores or small cracks in the the unburned propellant, where the local confinement can cause the pressure to become very high locally, the combustion front speeds up to shock wave speed with a low-pressure differential and it then accelerates further to a strong, fast, high-pressure shock wave, characteristics of detonations.

The same material may burn or detonate depending on the chemical formulation, the type and intensity of the initiation, the degree of confinement, the physical propellant properties and the geometric characteristics of the motor.[28, 1]

- Upper pressure limit

  If the absolute pressure and the pressure-rise rate become extremely high, some propellants will detonate. These pressures are above approximately 1500 MPa for some propellants,however, for others they are lower, near 300 MPa. They represent an upper pressure limit beyond which a propellant should not operate.[1]

- Toxicity

  A large share of all rockets do not have a significant toxicity problem, nevertheless, the chlorine in the oxidants of solid boosters produces hydrogen chloride and particulates than can be dangerous, launch vehicle boosters are fired close to the ground, consequently, most of the exhaust is dispersed over a wide area of the launch site. However, toxicity lays not only in the exhaust gases, a number of propellant ingredients, e.g., some cross-linking agents and burning rate catalysts and a few of the plastics used in fiber-reinforced cases can be dermatological or respiratory toxins, and even a few are carcinogens.[1, 31]

The basic solid propellant consists of two or more chemical components, or ingredients, that are categorised by major function, such as oxidiser, fuel, binder, plasticiser, curing, additives, and so on, each category described in the remainder of this section.

- Inorganic Oxidisers

  Ammonium perchlorate, due to its compatibility with other propellant materials, good performance, quality, uniformity and availability, is the most widely used crystalline oxidiser in solid propellants. Other solid oxidisers such as potassium nitrate, or saltpetre, which is used in gunpowder, is still being used but to a large extent have been replaced by more modern propellants containing ammonium perchlorate.

The oxidising potential of the perchlorates is generally high, which gives these propellants high specific impulses. Both ammonium and potassium perchlorate are only slightly soluble in water, a favourable trait in propellant use. All the perchlorate oxidisers produce hydrogen chloride and other toxic and corrosive chlorine compounds in their reaction with fuels.

The inorganic nitrates are relatively low-performance oxidisers compared with perchlorates, nevertheless, ammonium nitrate is used in some applications because of its low cost and smokeless and relatively non-toxic exhaust.

In the table 2.3 are some of the thermochemical properties of several oxidisers and oxygen radical containing compound.[28]

Table 2.3: Comparison of crystalline oxidisers.[28]

Oxidizer	Chemical Symbol	Molecular Mass (kg/kg-mol)	Density (kg/m^3)	Oxygen Content (wt%)	Remarks
Ammonium percholrate	NH_4ClO_4	117,49	1949	54,5	Low n, low cost, readily available.
Potassium percholrate	$KClO_4$	138,55	2519	46,2	Low burning rate, medium performance.
Sodium perchlorate	$NaClO_4$	122,44	2018	52,3	Hygroscopic, high performance.
Ammonium nitrate	NH_4NO_3	80	1730	60	Smokeless, medium performance.
Potassium nitrate	KNO_3	101,1	2109	47,5	Low cost, low performance.

- Fuels

  Powdered spherical aluminum is the most common fuel. During rocket combustion this fuel is oxidised into aluminum oxide, this aluminum increases the heat of combustion, the propellant density, the combustion temperature and consequently the specific impulse.

  Boron is a high-energy fuel that is lighter than aluminum and has a high melting point,$2304°C$. It is difficult to burn with high efficiency in combustion chambers of reasonable length. However, it can be oxidised at reasonable efficiency if the boron particle size is very small.

  Beryllium burns more easily than boron and improves the specific impulse of a SPRM, usually by about 15 seconds, however, its oxide have highly toxic powders, making its application unlikely.

  Aluminum hybride and beryllium hybride are, theoretically, attractive fuels due to their high heat release and gas-volume contribution, however, they are both difficult to manufacture and both deteriorate chemically during storage, with loss of hydrogen. Thus, the compounds are not used today in practical fuels.[28]

- Binders

  The binder provides the structural glue or matrix in which solid granular ingredients are held together in a composite propellant, having a primary effect on motor reliability, mechanical properties, propellant processing complexity, storability, ageing and costs. The raw materials are liquid pre-polymers or monomers. Hydroxyl-terminated poly-butadiene has been the favourite binders in recent years because they allow higher solid fraction and relatively good physical properties at the temperature limits. Binder materials are also fuels for SPRMs and are oxidised in the combustion process.[28]

- Burning-rate catalysts

  A burning-rate catalyst, e.g., iron oxide, lead stearate, or lithium fluoride, helps to accelerate or decelerate the combustion at the burning surface and increases or decreases the value of the propellant burning rate, allowing the tailoring of the burning rate to fit a specific grain design and thrust-time curve.[28]

- Plasticisers

  A plasticiser is generally a relatively low-viscosity organic ingredient which is also a fuel. It is added with the purpose of improve the elongation of the propellant at low temperatures and to improve processing properties, such as lower viscosity for casting or longer pot life of the mixed but uncured propellants.[28]

- Curing agents

  A curing agent or cross-linker, used only in composite propellants causes the binder to solidify. Although these materials constitute $0,2$ to 3% of the propellant mass fraction, a minor change in the percentage will have a major effect on the propellant physical properties, such as manufacturability and ageing.[28]

- Organic Oxidisers

  Organic oxidisers are explosive organic compounds with NO_2 radical or other oxidising fractions incorporated into the molecular structure. They can be crystalline solids, such as the nitramines HMX or RDX, fibrous solids such as nitrocellulose, or energetic plasticiser liquids such as nitroglycerine or diethylene glycol dinitrate. These materials can react or burn by themselves when ignited with enough activating energy but all of them are explosives and can also be detonated under certain conditions.[28]

- Additives

  Small amounts of additives are added to the solid propellant for various purposes, including, improving the physical properties, limiting migration of

chemical species from the propellant to the binder or vice-versa, minimizing the slow oxidisation or chemical deterioration during storage, improving the ageing characteristics or the moisture resistance, and accelerating or lengthening the curing time.

Bonding agents are additives to enhance adhesion between the solid ingredients and the binder. Stabilisers are intended to minimise the slow chemical or physical reactions that can occur in propellants. Desensitizing agents are used to make a propellant more resistant to inadvertent energy stimulus. Lubricants aid the extrusion process. Adding opaqueness, a common additive, to a transparent propellant prevents radiation heating at places other than the burning surface.[31]

Combustion of Solid Propellants

The combustion in a solid propellant involves complex reactions in the solid, liquid and the gas phases of a heterogeneous mixture. However, the physical and chemical processes occurring during the combustion are not yet totally understood, and the available analytical combustion models are oversimplified.

According to visual observations and measurements, the structure of the flame is different according to the type of solid propellant.

Occasionally, it is necessary to extinguish the burning of a SPRM before the consumption of all the propellant for multiple purposes[28]:

1. When a flight vehicle has reached the desired flight velocity or a precise total impulse cut-off is needed;

2. When it appears that a flight test vehicle will unexpectedly fly out of the safe boundaries of a flight test range facility;

3. To avoid collisions of stages for multi-stage flight vehicles during a stage separation manoeuvre;

4. When it is necessary to examine a partially burned motor.

The common mechanisms for achieving extinction are presented below:[18]

1. Very rapid depressurisation, usually by a sudden, large increase of the nozzle throat area or by a fast opening of additional gas escape areas or ports;

2. The motor operation is stopped when the flames are quenched by injecting an inhibiting liquid, e.g, water. Adding a detergent to the liquid allows a better contact with the burning surface and reduces the amount of liquid needed for quenching;

3. Lowering the combustion pressure below the pressure deflagration limit, in comparison with item 1, this depressurisation occurs slowly. Several solid propellants have a low-pressure combustion limit of $0,05$ to $0,15$ MPa, meaning that some propellants will not extinguish when vented during a static sea-level test at 1 atm ($0,1$ MPa) but will stop burning if vented at high altitude.

There are two combustion instabilities, both of them presented below[28]:

- Acoustic Instabilities

  When a SPRM experiences unstable combustion, the pressure in the interior gaseous cavities, made up by the volume of the port or perforations, fins, slots, conical or radial groves, oscillates by at least 5% and often by more than 30% of the chamber pressure. When instability occurs, the heat transfer to the burning surfaces, the nozzle and the insulated case walls is greatly increased. The burning rate, chamber pressure and thrust are also usually increased. However, consequently, the burning duration is decreased.

  In SPRMs the geometry of the oscillating cavity increases in size as burning proceeds and there are stronger damping factors, such as solid particles and energy-absorbing viscoelastic materials. The combustion cavity of a SPRM is a low-loss acoustical cavity containing a very large acoustical energy source, where a small fraction of the energy released by the combustion process itself can drive pressure vibrations to an unacceptable level.

  Combustion instability can occur spontaneously, often at some particular time during the motor burn period and the phenomenon is usually repeatable in identical motors. Figure 2.9 shows a pressure-time profile with typical instability. The pressure oscillations increase in magnitude as the thrust and the burning rate. The dashed lines show the upper and lower boundaries of the high-frequency pressure oscillations, and the dot-dash curve is the behaviour without instability after a slight change in propellant formulation. The vibration period shows a rise in the mean pressure.

  The propellant characteristics have strong effect on the susceptibility to instability. Changes in the binder, particle-size distribution, ratio of oxidiser to fuel and burn-rate catalysts can all affect stability, often in manners that are not predictable. All solid propellants can experience instability, however, in general, combustion instability problems do not occur frequently and when they do occur, it is rarely the cause for a drastic sudden failure or disintegration. Nevertheless, drastic failures have occurred.

- Vortex-shedding instability

  This vortex-shedding phenomenon only occurs with particular types of grains, and is associated with the burning on the inner surfaces of slots in the grain. Large segmented rocket motors have slots between segments, and some grain

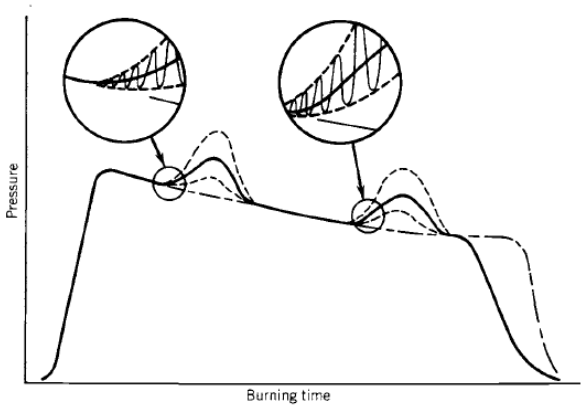

Figure 2.9: Simplified diagram showing two periods of combustion instability in the pressure-time history.[28]

configurations have slots that intersect the centerline of the grain. Figure 2.10, where heavy lines identify the burning surfaces, shows that hot gasses from the burning slot surfaces enter the main flow in the perforation or central cavity of the grain. The hot gas from the slot is turned into a direction toward the nozzle. The flow from the side stream restricts the flow arising from the upstream side of the perforation reducing the port area. This restriction causes the upstream port pressure to rise. The interaction of the two subsonic gas flows causes the formation of vortices. The shedding of these vortices can induce flow oscillations and pressure instabilities. The vortex shedding patterns can interact with the acoustic instabilities. The solution is to apply inhibitors to some burning surfaces or to change the grain geometry, e.g., by increasing the width of the slot, the local velocities are reduced and the vortices become less pronounced.

2.2.4 Propellant Grain and Grain Configuration

The grain is the shaped mass of processed solid propellant inside the rocket motor. The propellant material and geometrical configuration of the grain determine the motor performance characteristics. The propellant grain is a cast, molded, or extruded body. There are two methods of holding the grain in the case, as seen in figure 2.11.

Here, the liner is a sticky non-self-burning thin layer of polymeric-type material that is applied to the cases prior to casting the propellant in order to promote good bonding between the propellant and the case or the insulator.

Cartridge-loaded or free-standing grains are manufactured separately from the

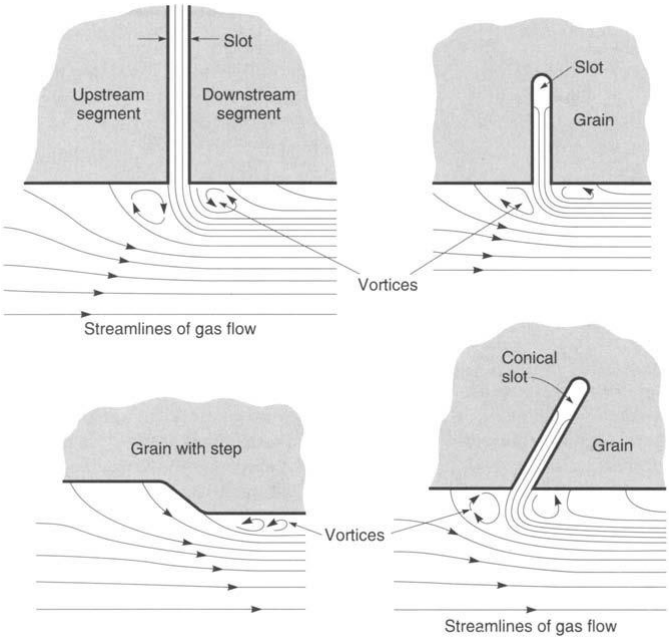

Figure 2.10: Sketches of four partial grain sections each with a slot or a step.[28]

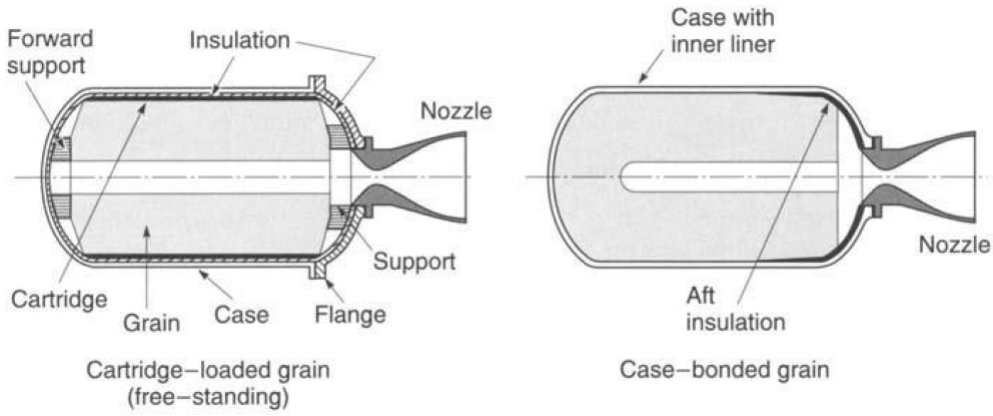

Figure 2.11: Simplified schematic diagrams of a free-standing and a case-bonded grain.[28]

case, by extrusion or by casting into a cylindrical mold or cartridge, and then loaded into or assembled into the case. This method is used in small tactical missiles and a few medium-sized motors. In case-bonded grains the grain is used as a mold and the propellant is cast directly into the case and is bonded to the case or case insulation. Free-standing grains can more easily be replaced if the propellant grain has aged excessively. Today almost all larger motors and many

tactical missile motors use case-bonding.

The shape or geometry of the initial burning surfaces of a grain has an influence on the pressure-time profile, as shown in figure 2.12.

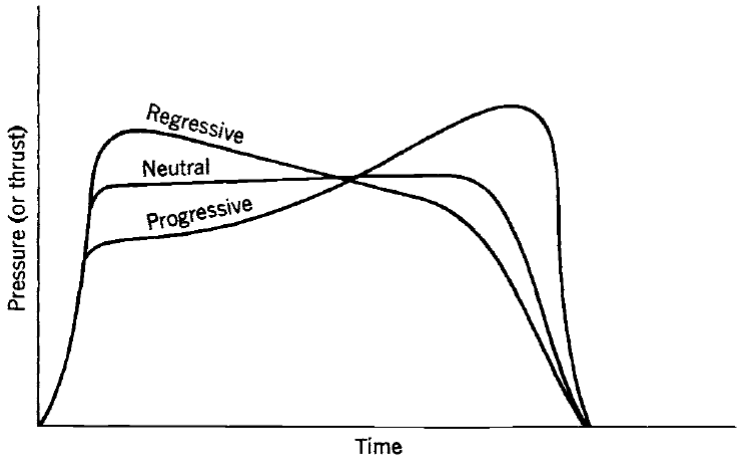

Figure 2.12: Classification of grains according to their pressure-time characteristics.[28]

This pressure or thrust profiles can be obtained by the following grain configurations:

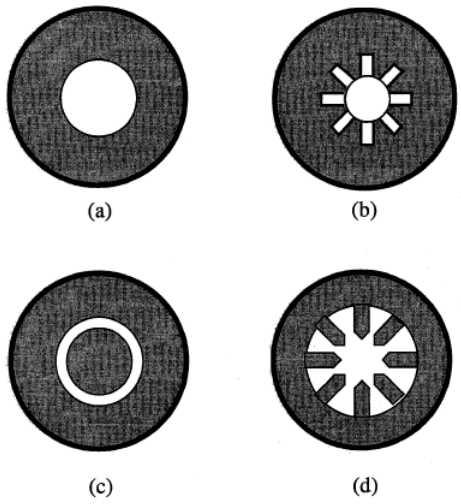

Figure 2.13: Cross-sections of grains.[31]

Where:

a - Called "progressive", here the circumference of the circular cross-section increases linearly with time, as does the area of the burning surface, and there is an increase in mass flow rate and hence in thrust;

b - Produces a quasi-constant thrust, i.e, "neutral", because the initial burning area is quite large due to the convolutions of the cog shape. As the cog "teeth" burn away the loss of burning area is compensated by the increasing area of the cylindrical part;

c - Also a "neutral" configuration, because burning takes place both on the outer surface of the inner rod and on the inner surface of the outer cylinder. The decrease in burning area of the outer surface of the rod is exactly compensated by the increasing burning area on the inner surface of the cylinder. However, this type of grain profile is difficult to manufacture and sustain due to the need to support the rod through the hot gas stream;

d - The narrow fins of propellant initially produce a very high surface area, so the thrust is initially very high. Once they have burned, a low and slowly increasing thrust is produced by the cylindrical section. When the diameter of the burning cross-section is large, the area changes more slowly than in the initial stages. Such a profile may be useful for strong acceleration followed by sustained flight, making this type of configuration is neither "neutral", "progressive" or "regressive".

There is a benefit to vehicle mass, flight performance, and cost in having a higher initial thrust during the "boost" phase of the flight, followed by a lower thrust during "the sustaining phase" of the flight. Grains which give this type of "regressive" thrust are shown in figure 2.14.[21, 31]

2.2.5 Integrity of the combustion chamber

The combustion chamber of a SPRM is also the fuel store and it is relatively large, in comparison, it is larger than the combustion chamber of a LPRM. Furthermore, since high thrust is usually the main requirement, the throat diameter is also larger. In modern rockets, the pressure experienced is about the same in both of them, about 50 bar. However, designing a large vessel to accommodate high pressure and high temperature is much more difficult than the equivalent task of designing a smaller vessel. The skin has to take the pressure and as the diameter increases, the thickness has also to increase, and because of the large surface area this has a major effect on the mass. In general, high-tensile steels are used.

In a SPRM as in a LPRM we need to ensure the thermal protection of the walls, the temperature of combustion is much higher than the softening point of most metals and the combustion products cannot be allowed to contact the walls for any extended period or disaster will occur. The best solution to avoid this situation is

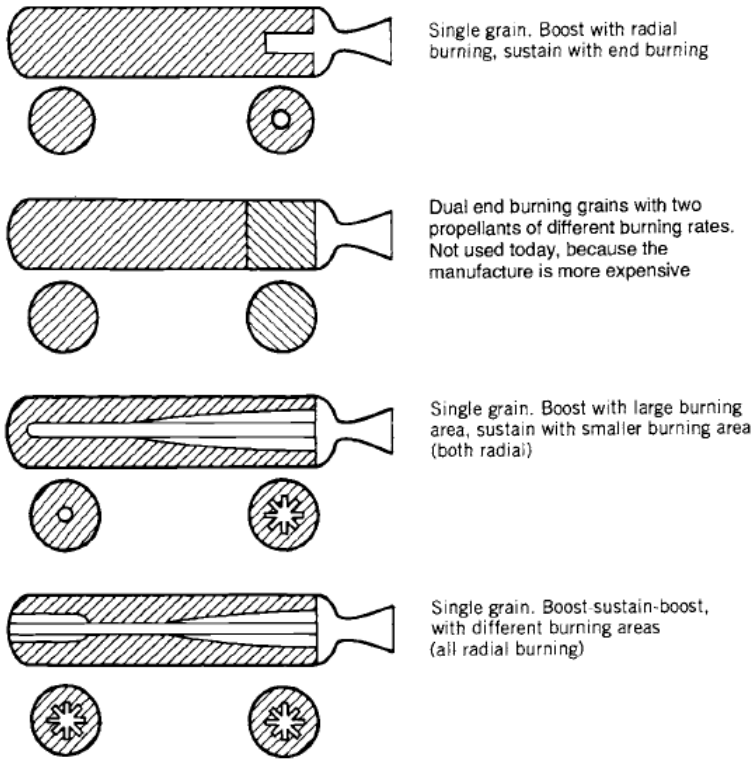

Figure 2.14: Grain configurations for an initial period of high thrust followed by a lower thrust period.[28]

to bond the propellant to the walls and to cover the remaining inside surfaces with a refractory insulating layer. This technique, case bonding, is used in most modern solid motors. The grain burns only in its inside surface so the propellant acts as an insulator. Boosters are normally used once and so any residual damage caused to the walls when the propellant is exhausted is not important. In fact, a thin layer of propellant usually remains after burn-out, sliver, due to the sudden drop in pressure which extinguishes the combustion. For potentially reusable casings and where particular care is required on manned missions, a layer of insulating material is also placed between the grain and the casing before it is bonded in, this method is called ablative cooling. The steel casing is covered with many layers of non-metallic material, as shown in figure 2.15, which have the purpose to provide good heat insulation, when undisturbed, and the purpose to slowly evaporate, or ablate, when exposed. This process extracts heat of vaporisation from the gas layers nearest the surface and forms an insulating cool gas layer. The materials used are combinations of silica fibres, phenolic resins and carbon fibres.

An external insulation can also be applied to the outside of the motor case with the purpose to reduce the heat flow from the air boundary layer outside the

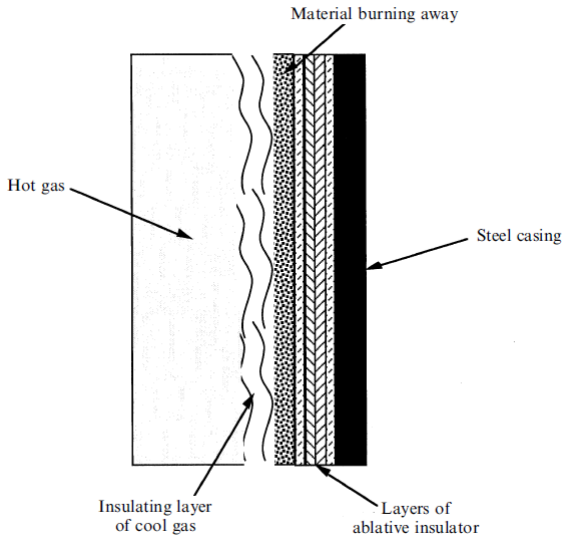

Figure 2.15: Thermal protection.[31]

vehicle which is aerodynamically heated to the case and then to the propellant. This technique is used specially in tactical missiles or launch boosters.

The joints between sections have to be gas tight and they also have to transmit the forces arising from the high thrust of the boosters. The combustion pressure of approximately 50 bar is sufficient to cause some deformation of the cylindrical sections so the joints must resist against this. Each section case is a cylinder with the wall as thin as possible, about 12 mm, to minimise mass. At each end there has to be a sturdy flange to take the fasteners and to properly transmit the forces to the cylindrical wall. Turning the whole section from solid material is a safe approach, however it is costly and other methods of forming the flanges can be employed, such as flow turning.

There are two kinds of joint between section, the factory joint and the field joint. The factory joint is assembled before the charge is installed and results from the need to make up large booster casings from steel elements of a manageable size. These joints can be protected by insulation before the grain is installed and are relatively safe. The field joint allows the booster to be assembled from ready-charged sections more or less at the launch pad. They have two safety issues: they are made under field conditions away from the factory; and they cannot be protected with insulation in the same manner as a factory joint because the two faces of the propellant charge come together on assembly which makes access to the inner surface of the joint impossible.

To ensure the nozzle thermal protection, both the nozzle and the throat are protected from the heat of the exhaust using similar techniques to those used to protect the casing. Here, the problem is more severe because of the high velocity

of the exhaust gases. The main structure of this components is made of steel but many layers of ablative insulator are applied to the inside. A heat sink is also used at the throat to reduce the transfer of heat to the steel structure. Most of the thrust is developed on the walls of the nozzle and so the structure needs to remain within its service temperature until burn-out. Ablation, heat diffusion into the heat sink and the thermally insulating properties of the throat lining keep the steel cool long enough to do its service. After burn-out it does not matter if the outer structure becomes too hot. Without such a lining the steel would reach its melting point in less than one second but the lining prolongs this by a factor of 200.[31]

2.2.6 Ignition Process and Hardware

A SPRM requires a stable and reliable ignition. Solid propellants ignition consists of a series of complex rapid events, which start on receipt of a a signal, usually electric, and include heat generation, transfer of the heat from the igniter to the motor grain surface, spreading the flame over the entire burning surface area, filling the chamber free volume, the cavity, with gas and elevating the chamber pressure. This must be accomplished without serious abnormalities such as over-pressures, combustion oscillations, damaging shock waves, hang-fires (delayed ignition), extinguishment and chuffing. The igniter is a SPRM generates the heat and gas required for motor ignition.

Motor ignition must usually be complete in a fraction of a second for all but the very large motors, the motor pressure rises to an equilibrium state in a very short time, as shown in figure 2.16.[28, 31]

For analytical purposes, the ignition process is conventionally divided into three phases:[28]

Phase I: Ignition time lag - The period from the moment the igniter receives a signal until the first bit of grain surface burns.

Phase II: Flame-spreading interval - The time from first ignition of the grain surface until the complete grain burning area has been ignited.

Phase III: Chamber-filling interval - The time for completing the chamber-filling process and for reaching equilibrium chamber pressure and flow.

The ignition will be successful once enough grain surface is ignited and burning so that the motor will continue to raise its own pressure to the operating chamber pressure. If the igniter is not powerful enough, some grain surfaces may burn for a short time, however, the flame will be extinguished.

Satisfactory attainment of equilibrium chamber pressure with full gas flow is dependent on:

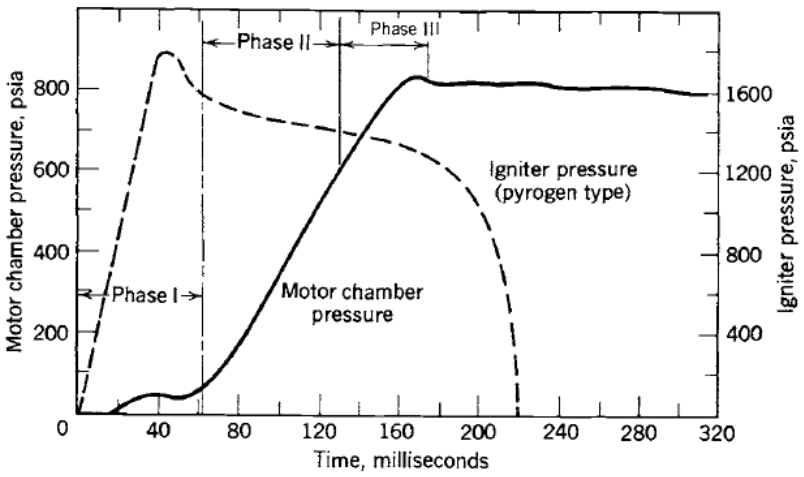

Figure 2.16: Typical ignition pressure transient portion of motor chamber pressure-time trace with igniter pressure trace. The electrical signal is received before time zero.[28]

1. Characteristics of the igniter and the gas temperature, composition and flow issuing from the igniter;

2. Motor propellant composition and grain surface ignitability;

3. Heat transfer characteristics by radiation and convection between the igniter gas and grain surface;

4. Grain flame spreading rate;

5. The dynamics of filling the motor free volume with hot gas.

The igniter propellant mass is small, habitually less than one percent of the motor propellant and burns typically at low chamber pressure so it has a small contribution to the motor overall total impulse. Thus, it is the designer's interest to reduce the igniter propellant mass and the igniter inert hardware mass to a minimum.

Observing the figure 2.17, we can see several alternative locations for igniter installations. When mounted on the forward end, the gas flow over the propellant surface helps to achieve ignition. With aft mounting there is little gas motion, particularly near the forward end, here the ignition must rely on the temperature, pressure and heat transfer from the igniter gas. And if mounted on the nozzle, the igniter hardware and its support is discarded shortly after the igniter has used all its propellants and there is no inert mass penalty for the igniter case.

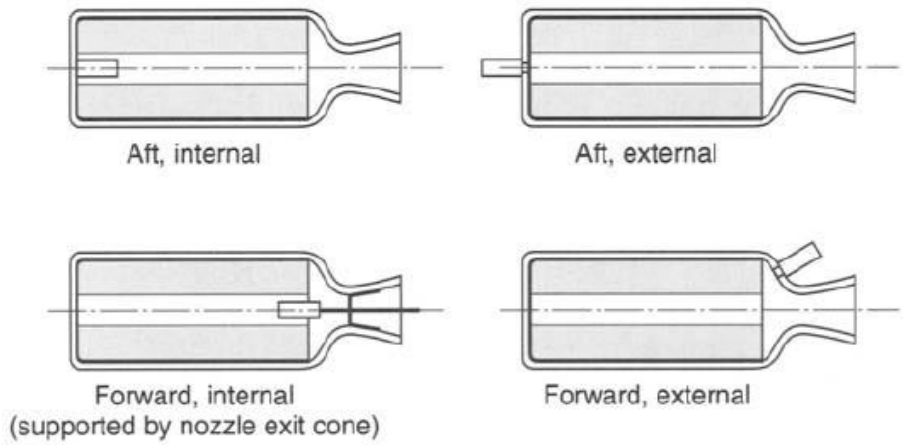

Figure 2.17: Mounting options for igniters. Grain configurations are not shown.[28]

Summarising, the requirements for an igniter propellant include the following:[28]

1. Fast high heat release and high gas evolution per unit igniter propellant mass to allow rapid filling of grain cavity with hot gas and partial pressurization of the chamber;
2. Stable initiation and operation over a wide range of pressures and smooth burning at low pressure with no ignition overpressure surge;
3. Rapid initiation of igniter propellant burning and low ignition delays;
4. Low sensitivity of burn rate to ambient temperature changes and low burning rate pressure exponent;
5. Operation over the required ambient temperature range;
6. Safe and easy to manufacture, safe to ship and handle;
7. Good ageing characteristics and long life;
8. Minimal moisture absorption or degradation with time;
9. Low cost of ingredients and fabrication.

So, in order to fulfil these requirements there are two basic types:[31, 18]

- Pyrotechnic igniters

  In industrial practice, pyrotechnic igniters are defined as igniters using solid explosives or energetic propellant-like chemical formulations as the heat-producing material. The ignition of the main charge, pellets, is accomplished by stages:

  1. The receipt of an electrical signal makes the initiator release the energy of a small amount of sensitive powdered pyrotechnic housed within the initiator, squib or the primer charge;
  2. The booster charge is ignited by heat released from the squib;
  3. The main ignition charge propellants are ignited.

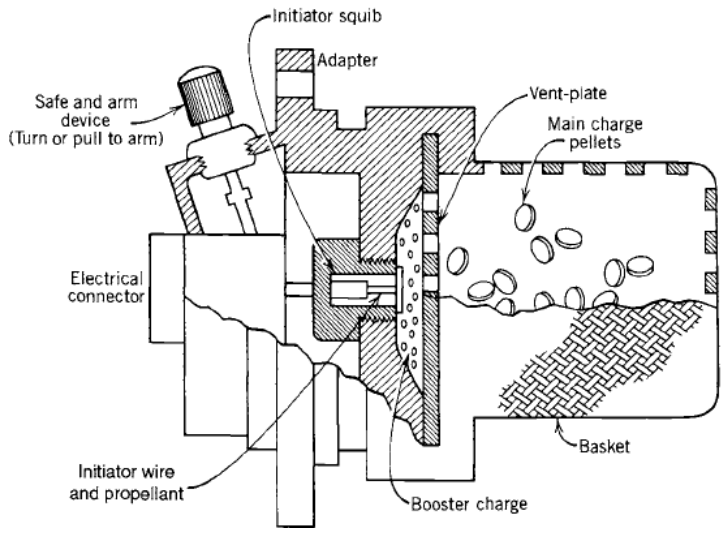

Figure 2.18: Typical pyrotechnic igniter.[28]

- Pyrogen igniters

  A pyrogen is basically a small rocket that is used to ignite a larger rocket motor. The pyrogen is not designed to produce thrust. All use one or more nozzle orifices, both sonic and supersonic types and most use conventional rocket motor grain formulations and design technology. Heat transfer from the pyrogen to the motor grain is largely convective with the hot gases contacting the grain surface. For pyrogen igniters the initiator and the booster charge are very similar to the designs used in pyrotechnic igniters. Reaction products from the main charge impinge on the surface of the rocket motor grain, producing motor ignition. It is a common practice on the very large motors to mount externally, with the pyrogen igniter pointing its jet

up through the large motor nozzle. In this case the igniter becomes a piece of ground-support equipment.

2.2.7 Multi-stage Rockets and Strap-on Boosters

Before accessing space, there was a dilemma that needed a solution: for optimum exhaust velocity, low in the atmosphere, the exhaust nozzle should be short, so that the exhaust does not expand too much. However, for vacuum the nozzle should be long and the exhaust should be expanded as much as possible.

The multi-stage rocket offers an ideal solution, the first stage can be designed for best performance in the lower atmosphere, while the upper stages can be designed to perform best in vacuum. This applies to the nozzle length and it can be applied to the type of fuel used.

It is easy to see that discarding the empty fuel tanks, as shown in the figure below, is bound to improve the performance of a rocket. The thrust remains the same, however, after the tanks have been dropped off, the mass of the rocket is smaller so the acceleration will be greater.

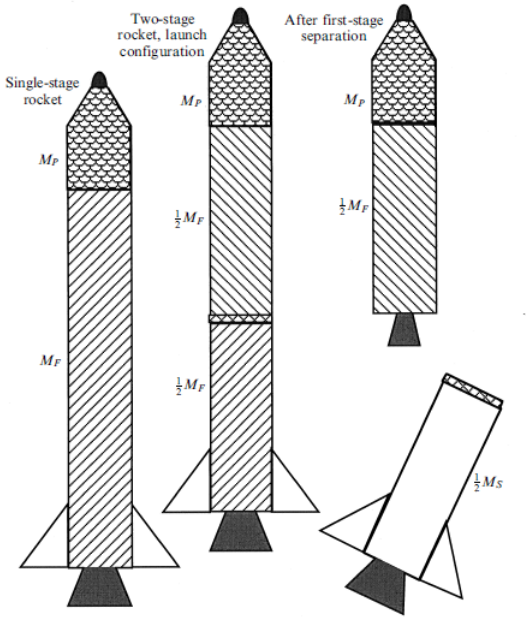

Figure 2.19: Multi-staging.[31]

Where:

- M_S - is the structural mass;
- M_F - is the propellant or fuel mass.

The first stage has the purpose of lifting the rocket more or less vertically through the lower atmosphere. It needs to have high thrust because it has to lift the entire mass of the multi-stage rocket. However, it cannot achieve a very high final velocity due to its adverse mass ratio, and because of atmospheric drag, which depends on the square of the velocity. The requirements suggest the use of large engines producing high thrust, as it is obvious that the thrust needs to be greater than the total weight of the rocket. Because the mass ratio and efficiency of the nozzle are so poor, the use of propellant combination giving high exhaust velocity is less important, meaning that less demanding propellants can be used, which simplifies the design and operation of the large first-stage engines. The upper stages are lighter and need less thrust, as the rocket is not working against gravity at the same extent, its path is now inclined so smaller engines can be used. Because the mass ratio and nozzle efficiency are increased, the use of propellants such as liquid oxygen and liquid hydrogen is beneficial, leading to high final velocity needed for injection into orbit. The multi-stage rocket thus leads itself to optimum engine design.

However, there is another technique, a variant on multi-staging, which began to be used in the USSR program, the archetypal three-stage rocket, Saturn V, quickly evolved into a two-stage rocket, with strap-on boosters. This technique has the advantage that the thrust of the first stage can be altered to account for an increased payload without changing the fundamental design of the main rocket. Up to six boosters were used with the R-7 rocket. Among modern launchers, the strap-on booster is a key feature, the largest being those used on the Space Shuttle and Ariane 5.

Boosters, which are usually solid-fuelled, can be used to improve the performance of a three-stage rocket, effectively making it a four-stage rocket or they can be used with a two-stage rocket, just as in the figure below. In both cases, the boosters are ignited at lift-off and burn for part of the first-stage operation. In modern launchers such as the Space Shuttle and Ariane 5, the first stage is optimised for high altitude and high mass ratio. This would produce insufficient thrust at low altitudes to lift the rocket off the launch pad and the nozzle, being optimised for high altitude, is also inefficient near sea level. The boosters provide the necessary high thrust for the early stages of flight.

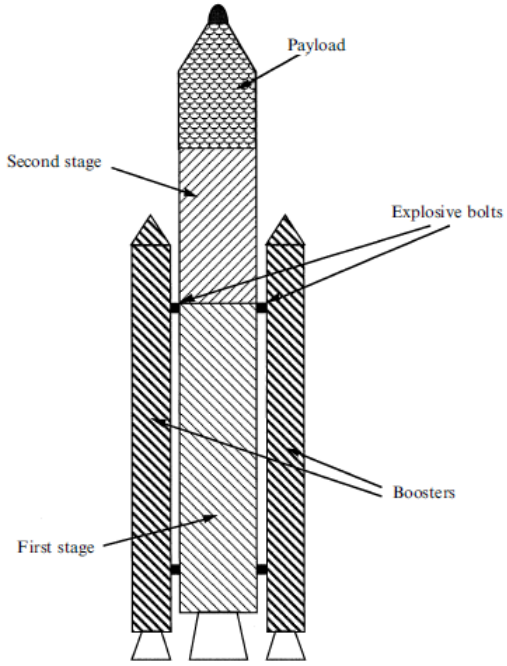

Figure 2.20: Launch vehicle with boosters.[31]

When the propellant is exhausted, the boosters are separated from the rocket by the firing of explosive bolts, which drives the nose of the booster away from the rocket axis. The lower attachment may also be released by means of explosive bolts or by a simple latch which releases once the booster axis has rotated through a certain angle. It is important that the booster does not collide with any part of the rocket during separation.

Boosters generally have a very high thrust and therefore a high mass-flow rate so they burn for a shorter time than the first stage.

There is a final element of the staging philosophy which has not been mentioned so far. The payload shroud or nose-cone as we can see in figure 2.20, is needed during the early part of the flight to protect the payload from atmospheric forces. At low altitudes these are the common forces of lift and drag which are experienced by aircraft and result in the requirement for streamlining. At higher altitudes, the rocket has reached a high velocity, much higher than the speed of sound, so the air is now very thin. The rapid motion of the air past the nose of the rocket now leads to heating. All these effects will damage the payload or require to be made more strongly than is consistent with its use in space. Thus, all launchers have a shroud around the payload to protect it. The satellite or spacecraft is in fact attached securely to the top of the last-stage motor and the shroud is mounted around it.

Once the rocket is sufficiently high in the atmosphere for aerodynamic and thermal effects to be negligible, the shroud is discarded and the launch continues with the payload exposed. To avoid damage to the payload during its operation the shroud splits in half and springs or explosive charges are used to safely abandon the two parts. The design of the shroud requires that it should have a low mass and that it should be able to withstand the heating and aerodynamics effects of high velocity. For heavy launchers it also has to provide a large enclosed volume in order to allow large spacecraft to be carried. These requirements normally lead to a composite construction for the shroud.[31]

2.2.8 Applications and Classification

As mentioned in chapter 1, rockets have a wide field of applications, so it is important to present examples of important applications.

- Space launch vehicles

  Since the first space launch in 1957 by the USSR thousands of space launch attempts have taken place, but unfortunately only a couple of hundreds were successful. Space launch vehicles or space boosters can be classified as expendable or recoverable/reusable or by the number of stages, size/mass of payloads or vehicles, manned or unmanned.

  Each space launch vehicle has a specific space flight objective, such as an earth orbit or moon landing. Typically it uses between two and five stages, multi-stage, depending on the specific space trajectory, the number and types of manoeuvres, the energy content of a unit mass of the propellant and other factors.

  The missions and payloads for space launch vehicles are many, such as:

Military - Reconnaissance satellites, command and control satellites;

N-M government - Weather observation satellites, GPS or geopositioning satellites;

Space exploration - Space environment, planetary missions;

Commercial - Communication satellites.

- Spacecraft

  According to their missions, spacecraft can be classified as earth satellites, lunar, interplanetary, trans-solar types and manned or unmanned spacecraft. The majority of spacecraft use liquid propellant engines, but the boosters that they use are generally of solid propellant. The Space Shuttle, which is actually a combination of launch vehicle, spacecraft and glider, uses two solid rocket boosters, as shown in the figure 2.21.[31]

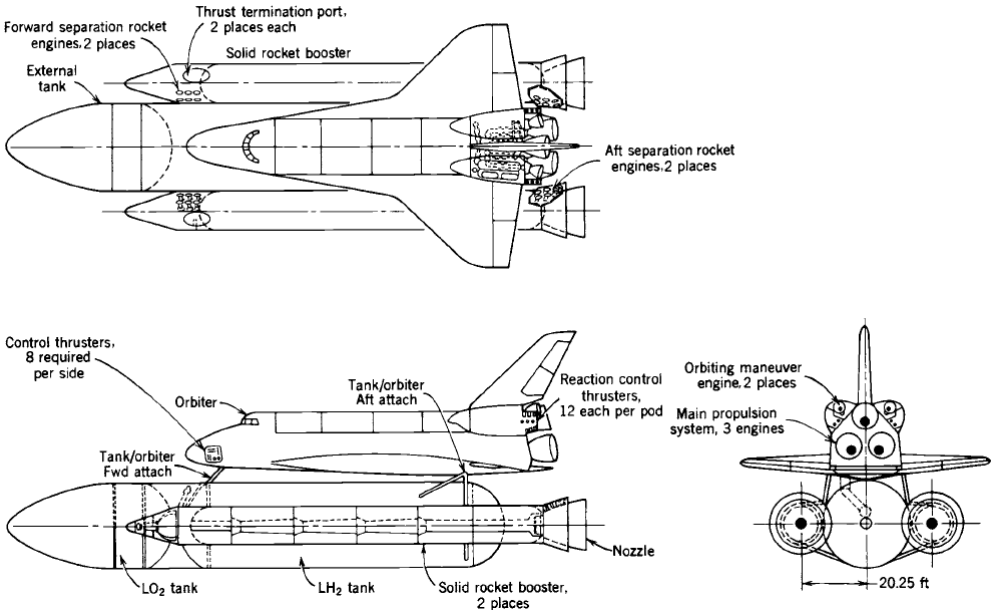

Figure 2.21: Simplified sketch of the Space Shuttle.[28]

- Missile and other applications

The largest part of all rocket systems built today are for military purposes, where the new Unites States new missiles uses now almost exclusively SPRM. The military missile classification is presented in the table 2.4, they can be strategic missiles, such as long-range ballistic missiles, 800 to 9000 km range, which are aimed at military targets within an enemy country, or tactic missiles, which are intended to support or defend military ground forces, aircraft or navy ships. The term surface launch can mean a launch from the ground, the ocean surface, from a ship, or from underneath the sea, submarine launch. Some tactical missiles, such as the air-to-surface SRAM missile, have a two-pulse SPRM, which is actually different form a multi-stage, where two separated insulated grains are in the same motor case. The time interval before starting the second pulse can be timed to the flight path or speed profile.

Table 2.4: Some United States missiles.[28]

Mission Category	Name	Propulsion
Surface-to-surface (long range)	Minuteman III	3 stages, solid
	Poseidon	2 stages, solid
Surface-to-air (or to missile)	Chaparral	1 stage, solid
	Improved Hawk	1 stage, solid
	Standard Missile	2 stages, solid
	Redeye	1 stage, solid
	Patriot	1 stage, solid
Air-to-surface	Maverick	1 stage, solid
	Shrike	1 stage, solid
	SRAM	2 staged grains
Air-to-air	Falcon	1 stage, solid
	Phoenix	1 stage, solid
	Sidewinder	1 stage, solid
	Sparrow	1 stage, solid
Antisubmarine	Subroc	1 stage, solid
Surface-to-surface (short range)	Hellfire	1 stage, solid
	Pershing II	2 stages, solid
	Tow	1 stage, solid
Cruise missile (subsonic)	Tomahawk	solid booster + turbofan

Other applications of SPRM are primary engines for research airplanes, assist-take-off rockets for airplanes, ejection of crew escape capsules and stores, personnel "propulsion belts", and propulsion for target drones, weather sounding rockets, signal rockets, decoy rockets, spin rockets, vernier rockets, underwater rockets for torpedoes and missiles and the throwing of lifelines to ships.[28]

2.2.9 Advantages and Disadvantages

Considering the complexities of the LPRM, the SPRM presents itself as a simple, easy to operate design and ready to operate rocket, so, it does not seem impressive that so much focus has been given to its design and development.

The solid propellant is storable for 5 to 25 years and can be designed for recovery, refurbishing and reuse and is relatively safe to handle. No propellant delivery system is required and this produces a huge improvement in reliability and cost.

The relative simplicity of a SPRM encourages its use for such purposes as weapons and strap-on boosters rockets to very large orbiting rockets. The relatively low exhaust velocity provided by solid rocket propellants does not create as great a penalty in the overall rocket mass needed for missions requiring relatively small vehicle velocity changes as it does for missions requiring large velocity changes.

With the development of heavily aluminized solid propellants, the propellant density has been greatly increased, leading to the production of rockets with very small cross sections and hence much reduced drag. Such an advantage is particularly important for low-altitude weapons use. Recently, also propellants with a high surface burning rate have been developed, with the result that it is relatively easy to design SPRM with enormous thrust-to-weight ratios.

However and obviously, the SPRM also presents disadvantages. The motor cannot be controlled once ignited, although the thrust profile can be pre-set, and the specific impulse is rather low because of the low chemical energy of the solid propellant. And although it is relatively safe to handle, the explosion and fire potential is larger and many require environmental permit and safety features for transport on public means of transport.

The exhaust gases are usually toxic for certain categories of composite propellants, e.g., propellants containing ammonium perchlorate. If the propellant contains more than a few percent particulate carbon, aluminium, or other metal, the exhaust will be smoky and the plume radiation will be very intense.

As for the LPRM, screaming instabilities continue to be of development concern. The methods to reduce such instabilities, or their effects, include the use of resilient material and propellant grain cross-sectional shapes that reduce wave reflection.[21, 28]

Chapter 3

SPRM Internal Ballistics Analysis and Prediction

This chapter will present a definition and characterization of the main driving phenomena of the SPRM internal ballistics operative phases. Thus, the state of the art of the internal ballistics model to simulate a given SPRM and the turbulence models available in ANSYS FLUENT are given, with a description of the model used in the project.

3.1 Internal Ballistics

The SPRMs internal ballistics studies the internal flowfield conditions inside a SPRM during all its operative conditions, from the ignition to the burn-out, allowing to characterize and define the behaviour, performance and the missions capabilities of the motor.

The overall combustion time can be separated into three main different temporal phases, according to the relation between thrust and time, ignition transient, quasi steady state and tail off, each of characterized by different driving phenomena.[11]

1. Ignition transient

   The impingement of the igniter jets on the propellant surface causes the grain propellant ignition, with possible acoustic mode excitement due to the interaction between the jets and the bore chamber geometry. The flame spreading triggers the ignition of the entire grain propellant surface, causing a greater and greater mass addition from the propellant and consequent chamber pressure increasing. During this period, flame spreading interval, the igniter stops to produce mass in the bore and the nozzle throat seal rupture occurs and a pressure overpeak due to the erosive contribution to the burning rate, as enhancing mechanism of the grain propellant combustion process, and to the

igniter mass flow rate in the bore often occurs. After the burning surface is completely ignited, the chamber filing and quasi steady state conditions are reached.

Consequently, a model able to describe the ignition transient must account the strongly unsteadiness of this phenomena, in terms of fluids dynamics, the heating and the mixing of gases into the bore, pressurizing gas, igniter gas products and grain combustion products. The grain variation geometry, due to the combustion, of this operative phase can be totally neglected so that the initial bore geometry can be considered fixed at its initial configuration.[11]

2. Quasi steady state

   In this operative phase the internal ballistics is mainly led by the grain mass addition and its variation in time due to grain combustion and burning surface recession and evolution in time. Nevertheless, even the nozzle throat geometry variation cannot be neglected. This event is due to the erosion-ablation phenomena to which the convergent zone and the throat section are subjected.

   During this phase, acoustic instabilities can cause low level, but sustained, pressure and thrust oscillations in the chamber due to vortex shedding phenomena.

   To describe all these phenomena, even because, of the possible presence of vortex shedding, a completely unsteady chamber dimensional, not 0-D, model is necessarily required.[11]

3. Tail off

   As the burning surface recedes and decreases in time, larger and larger parts of the liner and the case thermal protections are exposed to the action of the chamber hot gases. As a consequence, they are heated and because of ablative phenomena, begin to add ablation products in the chamber. As the grain combustion products mass addition into the chamber becomes smaller and smaller, a rapid decrease of the chamber pressure occurs, and combustion fluctuations and sliver generation can also occur.

   This operative phase is, therefore, characterised by unsteady events, related to the chamber pressure decrease in time, mixing of gases coming from the residual grain propellant combustion and case thermal protections ablations. Thus, they need to be described correctly by an accurate burning surface evolution evaluation.[11]

The objective of the internal ballistics is to provide the SPRM a propellant grain that will evolve combustion products consistent with the thrust-time schedule required for the mission. In order to achieve this objective, some parameters of the

rocket motor, called ballistics parameters need to be considered. A list of these ballistics parameters are presented and explained in the following section.

3.1.1 Ballistics Parameters

To present the following equations of the ballistics parameters and the basic thermodynamic principles, it is necessary to assume a concept which treats the rocket as an ideal heat engine. This ideal heat engine is based on the the following assumptions:[21, 31, 28, 2, 4, 27]

1. The gaseous products of combustion obey the perfect gas laws and are homogeneous;
2. The specific heat of the products of combustion is constant;
3. One-dimensional flow can be assumed. All exhaust gases leaving the rocket have an axially directed velocity;
4. There is no friction and all boundary layer effects are neglected;
5. There is no heat transfer to the walls, hence the flow is adiabatic;
6. Combustion is complete before the gas enters the nozzle;
7. The process is steady in time; There are no shock waves or discontinuities in the nozzle flow;
8. The gas velocity, pressure, temperature and density are all uniform across any sectional normal to the axis.

At figure 3.1 the external pressure acts uniformly on the outer surface of a rocket and the gas acts on the inside of the rocket, in this figure we can also see the geometrical positions of the throat.

- Thrust

  The thrust of a SPRM is the force produced by a rocket propulsion system acting upon a vehicle. It is the main design constraint of the propulsion system. A general and simple definition can be presented; it is the reaction experienced by its structure due to the ejection of matter at high velocity. Thrust can be calculated from momentum equation applied on the overall rocket system:

  $$T = \dot{m}u_e + (p_e - p_a)A_e \tag{3.1}$$

  Or:

  $$T = \dot{m}C \tag{3.2}$$

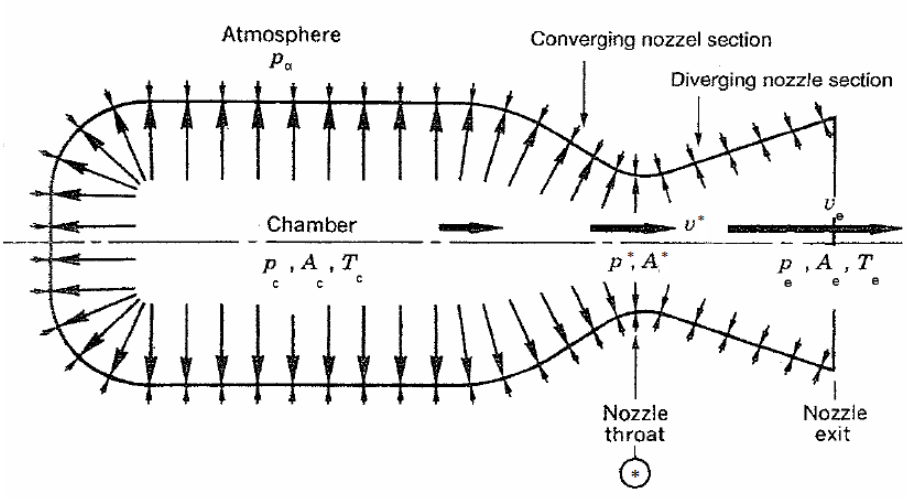

Figure 3.1: The influence of pressure of the surrounding fluid in rocket thrust.[31]

After some manipulation, this leads to:

$$T = p_c A^* \left\{ \frac{2\gamma^2}{\gamma - 1} \left(\frac{2}{\gamma + 1} \right)^{(\gamma+1)/(\gamma-1)} \left[1 - \left(\frac{p_e}{p_c} \right)^{(\gamma-1)/\gamma} \right] \right\}^{1/2} + p_e A_e - p_a A_e \tag{3.3}$$

The cross-sectional area of the throat of the nozzle, A^*, is an important parameter of the rocket motor, being in effect a measure of the size. The index γ is the ratio of the specific heat of the exhaust gases at constant pressure to that at constant volume. For rocket exhaust gases at high temperature the typical value is $\gamma = 1,2$. γ is related to the specific heat (c_p), the universal gas constant (R) and the molecular weight of the exhaust gases ($\mathfrak{M}$) by:

$$c_p = \frac{\gamma}{(\gamma - 1)} \frac{R}{\mathfrak{M}} \tag{3.4}$$

- Effective exhaust velocity

  In a rocket nozzle, the actual exhaust velocity is not uniform over the entire exit cross-section and does not represent the entire thrust magnitude, hence the velocity profile is difficult to measure accurately. Thus, a uniform axial velocity C is assumed which allows a one-dimensional description of the problem. The effective exhaust velocity is defined by:

$$C = u_e + (p_e - p_a) A_e \tag{3.5}$$

- Specific impulse

The specific impulse, I_{sp}, is a measure of the impulse or momentum change that can be produced per unit mass of the propellant consumed, i.e., the ratio of thrust to the propellant weight flow per second, hence its importance in the determination of the propellant weight necessary to meet the ballistics requirements. The units of specific impulse are seconds and the equation relating specific impulse to exhaust velocity is:

$$I_{sp} = \frac{C}{g_0} \tag{3.6}$$

Where g_0 is the standard acceleration of gravity, $g_0 = 9,8067 ms^{-2}$.

- Total impulse

  It has been found that the total impulse, I_t can be accurately determined in testing by integrating the area under a thrust time curve. For this particular reason, the average specific impulse is usually calculated from total measured impulse and effective propellant mass. The total impulse is directly proportional to the total energy released by all the propellant of the propulsion system. The total impulse is defined as the integration of thrust, F, over the operation duration, t_b:

$$I_t = \int_0^{t_b} F\, dt = \overline{F} t_b \tag{3.7}$$

  Where $\overline{F}$ is an average value of thrust over the burning duration, t_b.

- Thrust Coefficient

  The thrust coefficient, C_F represents the performance of the nozzle for a fixed propellant configuration. Thrust coefficient is defined as the thrust divided by the chamber pressure, p_c and the throat area A^*.

$$C_F = \frac{F}{p_c A^*} \tag{3.8}$$

  The thrust coefficient C_F is a function of gas property γ, nozzle expansion ratio ε, the pressure ratio across the nozzle p_c/p_e and the pressure outside the nozzle p_a.

$$C_F = \left\{ \frac{2\gamma^2}{\gamma - 1} \left(\frac{2}{\gamma + 1} \right)^{(\gamma+1)/(\gamma-1)} \left[1 - \left(\frac{p_e}{p_c} \right)^{(\gamma-1)/\gamma} \right] \right\}^{1/2} + \left(\frac{p_e}{p_c} - \frac{p_a}{p_c} \right) \varepsilon \tag{3.9}$$

- Characteristic velocity

  Characteristic velocity c^* is a function of the propellant characteristics and combustion chamber design. It is independent of nozzle characteristics. The c^* is used in comparing the relative performance of different chemical rocket propulsion system designs and propellants. It is easily determined from measured data of $\dot{m}$, p_c, and A^*. It measures the efficiency of conversion of thermal energy in the combustion chamber into high-velocity exhaust gas. The c^* can be formulated as:

$$c^* = \frac{p_c A^*}{\dot{m}} \tag{3.10}$$

  It has the dimensions of a velocity (ms^{-1}) and is based on measurable quantities. The thermodynamic form is given by:

$$c^* = \left\{ \gamma \left(\frac{2}{\gamma+1} \right)^{(\gamma+1)/(\gamma-1)} \frac{\mathfrak{M}}{RT_c} \right\}^{-1/2} \tag{3.11}$$

  For plotting purposes, this parameter is often combined with the combustion parameter, $\sqrt{T_c/\mathfrak{M}}$. For solid propellants this value of combustion parameter is about 10. We note that the units are not given in the references, however, in chapter 4, a logical argument will allow us to give units to the dimension.

- Nozzle throat area and expansion ratio

  As we have seen, the size of the throat area, A^*, is one of the main parameters of rocket size. The defining property of the nozzle is the exit area, A_e, and the shape of the nozzle can be expressed in a dimensionless way as the expansion ratio, ε.

$$\varepsilon = \frac{A_e}{A^*} \tag{3.12}$$

  An alternative expression for the expansion ratio can be derived:

$$\frac{A_e}{A^*} = \left\{ \frac{\left(\frac{\gamma-1}{2}\right)\left(\frac{2}{\gamma+1}\right)^{(\gamma+1)/(\gamma-1)}}{\left(\frac{p_e}{p_c}2/\gamma\right)\left[1-\left(\frac{p_e}{p_c}\right)^{(\gamma-1)/\gamma}\right]} \right\}^{1/2} \tag{3.13}$$

- Chamber pressure and MEOP

  Chamber pressure is the gas pressure inside the combustion chamber during motor operation. In grain design process, usually a limit on maximum

pressure is established at the time grain design activity commences. Concurrent with grain design, the motor case and other structural components are being designed and analysed with this maximum pressure. This constraint on chamber pressure is usually named as "Maximum Expected Operating Pressure" (MEOP). The chamber pressure can be obtained using:

$$P_c = \left(\frac{a A_b \rho_b c^*}{A^*} \right)^{\left(\frac{1}{1-n}\right)} \tag{3.14}$$

- Burning rate

  The burning surface of a propellant grain recedes in a direction essentially perpendicular to the surface. The rate of regression, usually expressed in cm/sec, mm/sec, or in/sec, is the burning rate, r_b.

  Aside from the propellant formulation and propellant manufacturing process, burning rate in a full-scale motor can be increased by the following:

  1. Combustion chamber pressure.
  2. Initial temperature of the solid propellant;
  3. Combustion gas temperature;
  4. Velocity of the gas flow parallel to the burning surface;
  5. Motor motion (acceleration and spin-induced grain stress).

  The burning rate of propellant in the motor is a function of many parameters, and at any instant governs the mass flow rate, $\dot{m}$ generated and flowing from the motor:

$$\dot{m} = A_b r_b \rho_b \tag{3.15}$$

  Here A_b is the burning area of the propellant grain, r_b the burning rate, and ρ_b the solid propellant density prior to motor start. The total mass m of effective propellant burned can de determined by:

$$m = \dot{m} \int A_b r_b dt \tag{3.16}$$

  There are several quasi-steady formulations to predict the burning rate of an energetic solid material. One of them is the APN model, which is an empirical model suitable for composite propellants in the absence of a more suitable fundamental combustion model. The APN model approximates the burning rate as solely dependent on the mean local pressure using the Vielle's or Saint Robert's law:

$$r_b = ap_c^n \tag{3.17}$$

Where p_c is the chamber pressure, a in an empirical constant influenced by ambient grain temperature, also known as the temperature coefficient, and n is the burning rate exponent, or the combustion index, and it is independent of the initial grain temperature and describes the influence of chamber pressure on the burning rate.

The sensitivity of burning rate to propellant temperature can be expressed in the form of temperature coefficients, the two most common are:

$$\sigma_p = \left(\frac{\partial ln\ r_b}{\partial T}\right)_p = \frac{1}{r_b}\left(\frac{\partial r_b}{\partial T}\right)_p \tag{3.18}$$

and,

$$\pi_K = \left(\frac{\partial ln\ p}{\partial T}\right)_K = \frac{1}{p_c}\left(\frac{\partial p}{\partial T}\right)_K \tag{3.19}$$

Where σ_p is known as the temperature sensitivity of burning rate expressed as percent change of burning rate per degree change in propellant temperature at a particular value of chamber pressure. The second one π_K is known as the temperature sensitivity of pressure expressed as percent change of chamber pressure per degree change in propellant temperature at a particular value of K, which is the ratio of the burning surface area to throat area.

However, this model does not take into account the contribution of the erosive and dynamic burning.

The erosive burning effects become important in SPRMs with high gas cross-flow velocities and can strongly affect the SRPM internal ballistics and performances. They define, in fact, an increase on the quasi-steady burning rate, especially during the IT and also in the first part of the QSS, for certain SPRM configurations. These effects can heavily modify the combustion surface evolution in time and result in a early exposure to hot gases of parts of the motor case.

The erosive burning mechanism is believed to be caused by the increase in the gas to solid heat feedback and by the turbulence enhanced mixing and reaction of the oxidiser or fuel rich gases pyrolysed from composite propellants [20, 19].

A very simple and successfull used model for the erosive burning is the Lenoir and Robillard model [23], that considers the main cause of the effects related to an additional heat flux to the propellant.

The dynamic burning rate term represents a correction to the quasi-steady burning rate model, in order to account the effects of non-steady combustion processes, due in particular to unsteady phenomena occurring in the combustion chamber. Therefore, the effects of the dynamic burning must be expected to affect only transient phenomena of the SPRM internal ballistics, thus: the propellant ignition and initial pressurization during the IT, the TO phase and possible motor pulsing related to motor acoustic instability.

A simple model to describe the dynamic burning rate term is the Zel'dovich and Novozhilov model. It provides a simple way to represent the conductive heat feedback from the surface to the gas phase, that modify in some manner the grain propellant combustion processes.[23]

3.2 SPRM Models

There are many different numerical simulation models to simulate a given SPRM. They have different degrees of accuracy, bore chamber dimensional models and, commonly, prediction abilities restricted to temporal bounded operating intervals (IT, QSS and TO), related to the sub-models connected to the gas-dynamics model.

1. For the Ignition Transient: SPIT [7], KUO [3], MUG [9, 8], ROCSTAR [22, 32];
2. For the Quasi Steady State: PIBALL [12], SPP [13], ROCBALLIST [23], ROCSTAR, SPINBALL [11] and GREG [11];
3. For the Tail Off: PIBALL, SPP, ROCBALLIST, ROCSTAR.

The internal ballistics numerical simulations models mentioned above can even be classified according to their dimensional modelling type of the bore chamber flow-field:

- 0D quasi steady or unsteady models - PIBALL, SPP and ROCBALLIST 0-D;
- Q1D unsteady models - SPIT and KUO ROCBALLIST 1-D;
- 2D/3D unsteady models - MUG and ROCSTAR.

Consequently, for the analysis, study and prediction of SPRMs internal ballistics are used different numerical models for the Ignition transient and for the subsequent operative phases.

The numerical codes mentioned do not represent the complete list of existing internal ballistics codes. In fact, all the industries producing SPRM have their own-made proprietary models which are covered by industrial secret.[11]

3.3 ANSYS FLUENT Models

There are many turbulence models available in ANSYS FLUENT, the following list is a list of the available models.

- Spalart-Allmaras Model;
- Standard, RNG, and Realizable $k-\varepsilon$ Models;
- Standard and SST $k-\omega$ Models;
- $k-kl-\omega$ Transition Model;
- The V2F Model;
- The Reynolds Stress Model;
- Scale-Adaptive Simulation Model;
- Detached Eddy Simulation;
- Large Edddy Simulation Model;
- Embedded Large Eddy Simulation.

For more information about these turbulence models theory or how to use them, the reader must see references [5, 6].

3.4 RNG k-ε Model

The $k-\varepsilon$ with RNG (Renormalization Group Theory) model was chosen for this study. Default values were used to set up the model for the unknown values of the turbulent flow. The work by Thakre and Yang [30] and Moore [24] used the RNG turbulence model and similar values in modeling turbulence in a SPRM nozzle erosion investigation supporting the selection made in this study. This model accounts for a wide range of Reynolds number flow and more accurately accounts for rapidly strained flows, both of which occur in these models [6]. It is similar in form to the standard $k-\varepsilon$ model but includes the following refinements:

- The RNG model has an additional term in its ε equation that improves the accuracy for rapidly strained flows;
- The effect of swirl on turbulence is included in the RNG model, enhancing accuracy for swirling flows;
- The RNG theory provides an analytical formula for turbulent Prandtl numbers, while the standard $k-\varepsilon$ model uses user-specified, constant values;

- While the standard $k-\varepsilon$ model is a high-Reynolds number model, the RNG theory provides an analytically derived differential formula for effective viscosity that accounts for low-Reynolds number effects. Effective use of this feature does, however, depend on an appropriate treatment of the near-wall region.

These features make the RNG $k-\varepsilon$ model more accurate and reliable for a wider class of flows than the standard $k-\varepsilon$ model.[5]

A more comprehensive description of RNG theory and its application to turbulence can be found in [26].

Chapter 4

Results

This chapter is devoted to present the internal ballistics simulation, i.e., the SPRM studied in this thesis, the model set-up, which includes the computer design and the mesh construction, the results of the simulation and the validation of the same results, comparing the results with the results of other authors found in the bibliographical research.

4.1 NAWC Motor No.13

The Naval Air Warfare Center (NAWC) tactical motor no.13 (figure 4.1) was studied. It has a relatively simple conical shape of the grain propellant and a simple cylindrical case.

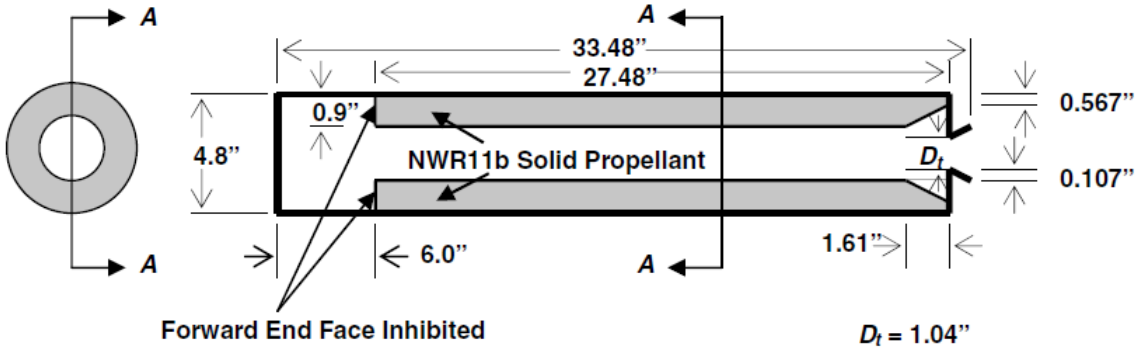

Figure 4.1: NAWC motor no.13 grain geometry (1 in.=2,54 cm).[23]

The propellant used in motor no.13 is the NWR11b propellant, its composition is reported in the table 4.1 and characteristics can be seen in chapter 2. It has a burning rate of $r_b = 0,541\ cm/s$ at $6,9\ MPa$, a burning rate exponent of APN

De Vieille Saint Robert of $n = 0,461$ and a density of about 1700 kg/m^3.

Table 4.1: NAWC motor no.13 propellant composition.[11]

Component	Mass Percentage
AP	83 %
HTPB	11.9 %
Oxamide	5 %
carbon black	0.1 %

In this composite propellant, AP is the oxidizer, HTPB is the binder, oxamide the fuel and the carbon black is used as an opacifier. The opacifier has the function of ensuring that the heat does not penetrate far below the surface of the grain, which could cause detonation. The opacifier also prevents sub-surface overheating and localized premature ignition in the grains where imperfections absorbing the thermal radiation are present. [11, 23, 29, 10]

4.2 Burning Surface

The area of each burning surface has been measured for each webstep, or burn distance. To measure this burning area, the propellant has been drawn in ANSYS FLUENT (Design Modeler), and the area has been calculated. A thin layer of unburned propellant, sliver, was assumed, $0,86$ mm. The results of the burning surface were compared with the results of Cavallini [11]. However, observing the results of Cavallini [11] we immediately noticed a disagreement, according to Wilcox et al. [23] the final webstep can only go $22,86$ mm, but in the work of Cavallini [11] the final webstep is $23,1141$ mm. Thus, the grain geometry followed was the one of Wilcox et al. [23]. For this reason, the results obtained, compared with the results of Cavallini [11], will show a discrepancy in the final webstep.

The burn distances are typically referred to as websteps. The webstep of a grain is the largest distance that a burning surface will travel.

The burning area was calculated for 11 websteps but, to approximate the data as continuous, a linear inter-polarisation was performed.

The results of the burning surface. The figure 4.2 shows the results obtained compared with the results of Cavallini [11] obtained with a numerical code, GREG.

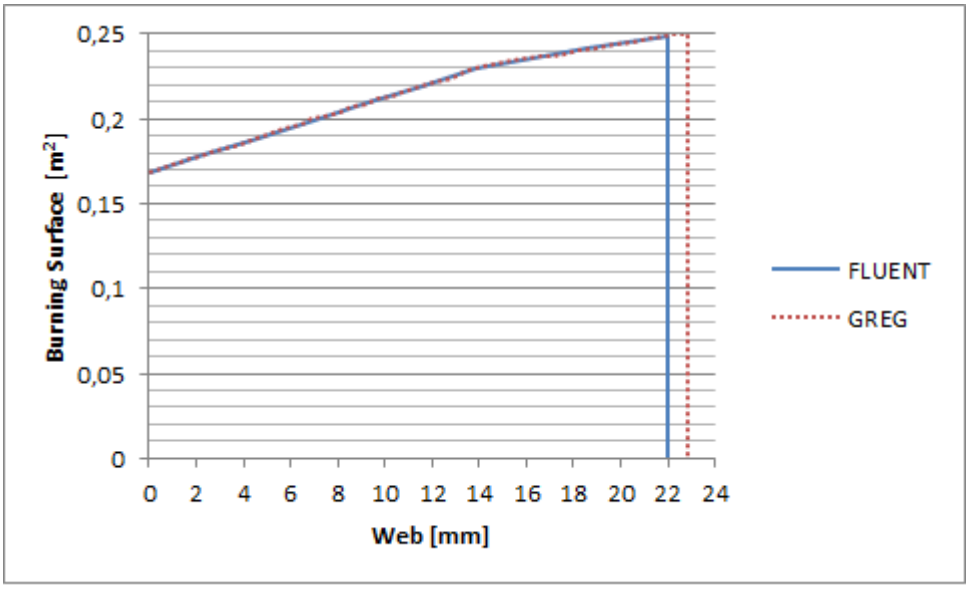

Figure 4.2: Burn area versus webstep.

Furthermore, we also can compare the results with the results of another numerical code, SPINBALL, that modelled the burning rate considering the contribution of the dynamic burning and also with or without the contribution of the erosive burning [11]:

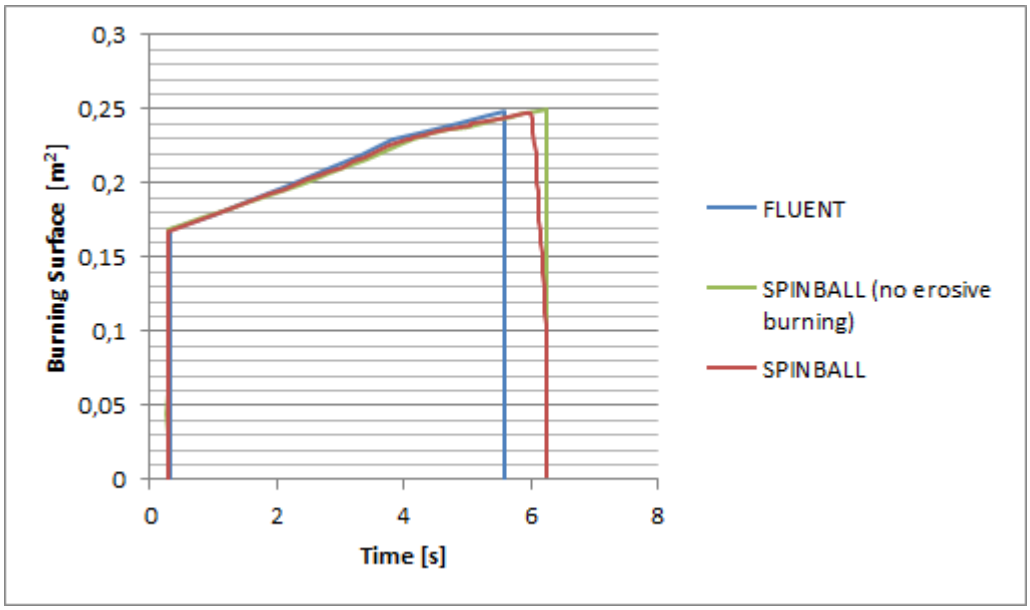

Figure 4.3: Burning surface.

Observing the results we conclude that the technique used for the calculation of the burning surface give satisfactory and robust results, thus validating our results.

4.3 Propellant Composition

The thermophysical properties of the grain propellant combustion products were evaluated starting from initial propellant composition with the Chemical Equilibrium with Applications program, available by NASA [15, 16]. The assumption made is the reaching of the chemical equilibrium condition for the combustion reactions, evaluated for some pressure values, in the pressure operative range of the motor, from about 1 to about 50 bars. No nozzle area variation is evidenced by the experimental results. Hence, a constant value of the nozzle throat diameter and a fixed nozzle configuration is considered during the internal ballistics simulation.

The results obtained are shown in table 4.2:

Table 4.2: Products of combustion in the chamber.

#	Mass Fraction
*CO	0,11558
*CO_2	0,16611
COOH	0,00001
*CL	0,05479
CLO	0,00065
CL_2	0,00038
*H	0,00072
HCL	0,20024
HNO	0,00001
HOCL	0,00019
HO_2	0,00012
*H_2	0,00339
H_2O	0,2239
H_2O_2	0,00001
*NO	0,01374
NOCL	0,00001
NO_2	0,00002
*N_2	0,11828
*O	0,00901
*OH	0,04127
*O_2	0,05157

Where * means that the thermodynamic properties are fitted to 20000 K.

The combustion gas has been treated as an ideal gas that respects the kinetic theory. However, since the mass fraction of $COOH$, H_2O_2 and $NOCL$ are small compared to the other mass fractions and since those components of the gas are not present in the FLUENT database, they were not included in the internal ballistics simulation.

4.4 Model Set-up

There are several assumptions made in order to set-up the CFD model:

1. No throat growth;
2. No deformation of the grain due to operating pressure and temperature;
3. No erosive burning;
4. No dynamic burning;
5. The motor grain ignites instantaneously;
6. Chemical reaction go to completion immediately upon combustion;
7. The combustion gas follows the Ideal Gas law;
8. Steady-state pressure predictions are calculated for each webstep;
9. The combustion gas is calorically perfect;
10. The combustion gas has constant properties;
11. The solid propellant has a combustion parameter of 10 $\sqrt{\frac{k^2 \times kmol}{J}}$;
12. The combustion gas respects the Kinetic theory.
13. The case wall of the motor is adiabatic.

The model created in ANSYS FLUENT uses the pressure based, implicit solver. It is set to 2-D axysymmetric reflecting the motor geometry and it is set to steady-state based on the assumptions above. The working fluid is viscous and it follows the ideal gas law so the energy equation is turned on.

The assumption that the case wall of the motor is adiabatic, i.e., no heat from the combustion is lost through the case walls as the SPRM burns is supported by the work of Moore [24].

4.5 Boundary Conditions

The insulated case is modelled as a stationary wall. It uses a no-slip condition and the default value for the wall roughness. The wall thermal conditions are defined using heat flux values. These values are set to zero in the adiabatic models.

Two boundary conditions include the centerline and the working fluid. The motor centerline is the x-axis about which the case, throat and grain geometries are rotated.

The grain surface is defined as a mass flow inlet boundary. The mass flow direction is specified as normal to the surface. Turbulence kinetic energy and dissipation rate are both set to zero as required in laminar, transpired flow [34].

The throat is defined as a pressure-far-field, where the Mach number is equal to 1 to make sure that we have supersonic flow in the nozzle. Turbulence kinetic energy and dissipation rate are both set to 1. The total temperature is equal to the flame temperature, 2300 K, as suggested by Cavallini [11].

The grain boundary mass flow for the individual model using the A_b data obtained by the Design Modeler in ANSYS FLUENT. Using the relationship between chamber pressure, p_c, and the grain surface area, A_b, in equation 3.14, the pressure is found for each webstep. This pressure is used to determine the mass flow off the grain only. The pressure reported in the final solution is obtained from FLUENT. Mass flow off the grain is found using equation 3.15. This value is calculated and used as the boundary condition for each webstep. Table 4.3 shows the results obtained for the several webstep constructed.

The external temperature and pressure are ambient, at 300 K and 101,325 kPa, respectively.

Table 4.3: Boundary condition pressure and time.

#	Webstep (m)	Burn Area (m^2)	Pressure chamber (Pa)	Burning rate (m/s)	Mass flow rate(kg/s)	Delta time (s)	Time (s)	Shifted (s)
1	0	0,168406	2481458,938	0,003378611	0,967263179	0	0	0,33
2	0,0023114	0,178577	2766670,802	0,00355239	1,07843767	0,650660592	0,6506606	0,98066059
3	0,0046281	0,188756	3066365,962	0,003724876	1,195257694	0,621953531	1,2726141	1,60261412
4	0,0069342	0,198604	3369784,596	0,003890476	1,313529114	0,592755163	1,8653693	2,19536928
5	0,0092456	0,209062	3706390,193	0,004065039	1,444736685	0,568604681	2,433974	2,76397397
6	0,011557	0,219231	4047807,983	0,004233568	1,57782003	0,545969686	2,9799437	3,30994365
7	0,0138684	0,229397	4402938,967	0,004400921	1,716248726	0,525208246	3,5051519	3,8351519
8	0,0161798	0,23548	4622004,966	0,004500544	1,801639813	0,513582346	4,0187342	4,34873424
9	0,0184912	0,2409356	4822640,138	0,004589576	1,879846633	0,503619557	4,5223538	4,8523538
10	0,0208027	0,2462248	5020901,906	0,004675613	1,95712831	0,494373648	5,0167274	5,34672745
11	0,022	0,2488948	5122381,957	0,004718943	1,996684845	0,253722046	5,2704495	5,6004495

To obtain the previous table, the following parameters were used:

- $A^* = 0,000548055\ m^2$
- $a = 3,8087e{-}6\ m^2 \times s/kg$;
- $n = 0,461$;
- $r_{b(ref.)} = 0,541\ cm/s$;
- $\rho_b = 17000\ kg/m^3$;
- $\gamma = 1,2$;
- $R = 8314,47\ J/(kmol \times K)$;

- $P_{c(ref.)} = 6,89\ MPa$;
- $\sqrt{T_c/\mathfrak{M}} = 10\ \sqrt{\frac{k^2 \times kmol}{J}}$;
- $c^* = 1406,004\ m/s$.

Because of the fact that the igniter performance is not simulated in this work, the simulated pressure traces have been shifted in time by an amount corresponding to the igniter behaviour, $0,33\ s$, to line up for experimental results, as suggested by Wilcox et al. [23].

4.6 Convergence Criteria

The CFD solutions had to meet or exceed convergence criteria. These criteria are defined for the residual monitor parameters in the mass flow between the grain, mass flow inlet and the exit plane. All websteps models are converged when the residuals are less than or equal to the values listed in table 4.4 and the mass imbalance between the mass flow off the grain and the mass flow out of the throat exit plane was less than the convergence criteria:

Table 4.4: Convergence criteria.

Residual	**Criterria**
Continuity	1,00E-03
Velocity in X-direction (axial)	1,00E-03
Velocity in Y-direction (radial)	1,00E-03
Energy	1,00E-06
k (turbulence)	1,00E-03
ε (turbulence)	1,00E-03
Mass imbalance	1,00E-03

4.7 Mesh Sensitivity

A mesh sensitivity study was performed to ensure acceptable solution accuracy while using computer time efficiently. The SPRM free volume was meshed for the first webstep. Several mesh sizes were tested until the results produced were considered reasonably insensitive to mesh density respecting the limits for the values of y^+ and y^*. The results for the different mesh sizes are shown in figure 4.4:

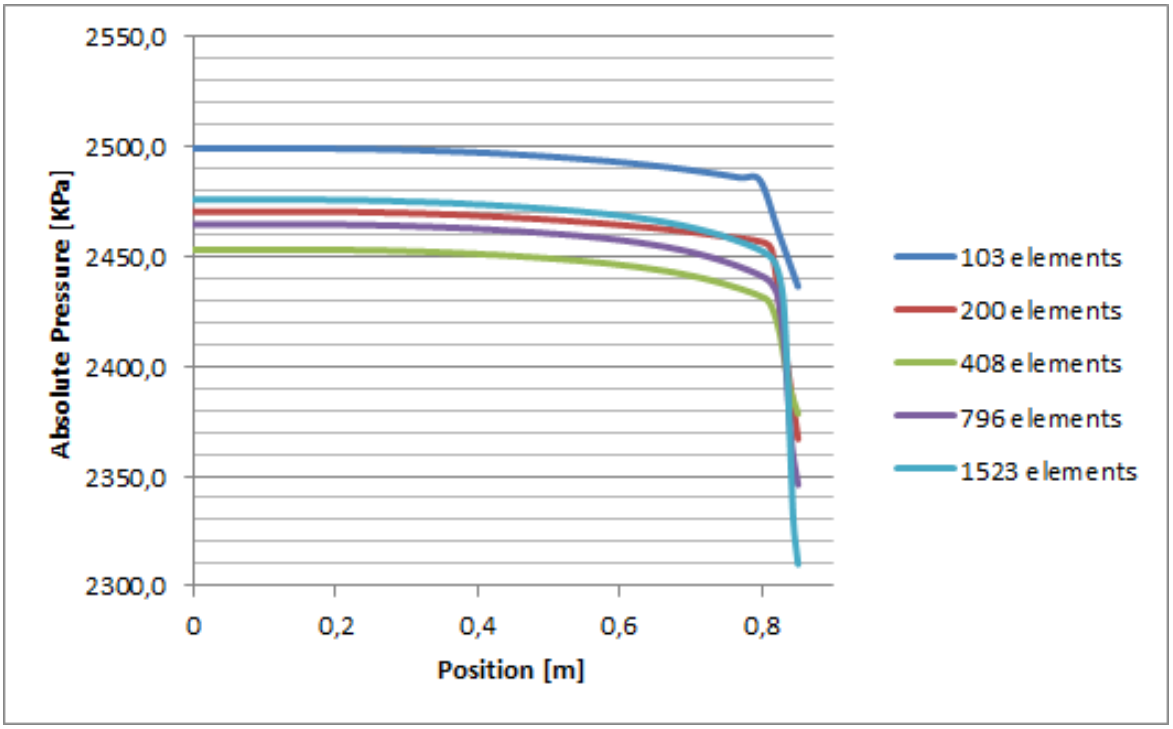

Figure 4.4: Mesh sensitivity study.

The number of elements was gradually increased in the x-direction and y-direction, respecting the equations below:

$$N_x N_y = N_{xy} \tag{4.1a}$$

$$\sqrt{2}N_x\sqrt{2}N_y = 2N_{xy} \tag{4.1b}$$

$$\sqrt{2}(\sqrt{2}N_x)\sqrt{2}(\sqrt{2}N_y) = 4N_{xy} \tag{4.1c}$$

To perform the sensitivity study of the mesh in order to reduce the number of approximations in the number of elements in the x-direction and in the y-direction, N_x and N_y, respectively, the starting number of elements of N_x and N_y was a power of 2.

The mesh selected for the internal ballistics was the one with 1523 elements which provided an overall agreement with the other studies, provided satisfactory results of chamber pressure as well as y^+ and y^* and used computational time efficiently. The mesh can be visualized in figure 4.5:

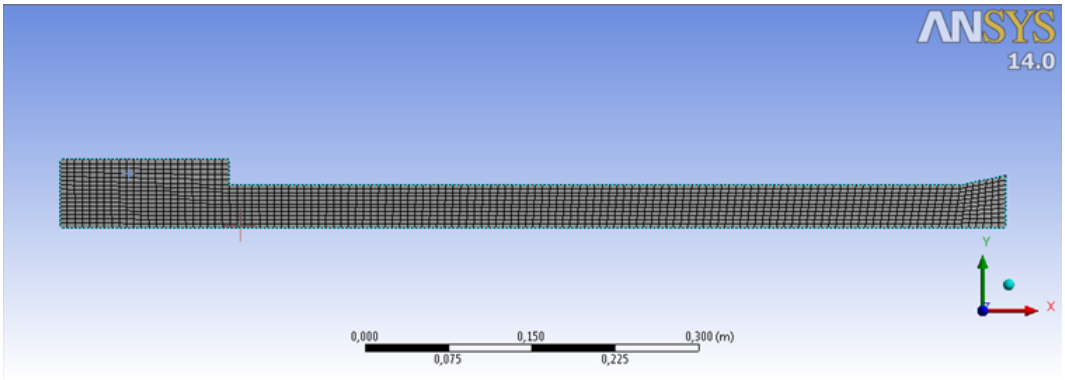

Figure 4.5: Generated mesh.

For this mesh:

- $y^+ = 42,976402$;
- $y^* = 133,1359$;
- $N_x = 128$;
- $N_y = 16$.

Therefore, we can conclude by the values of y^+ and y^* that the Law of the wall [33] is respected. Even though the volume of the meshed space would change for every webstep, the number of elements N_x and N_y was kept the same for all the webstep, $N_x = 128$ and $N_y = 16$. Therefore, the number of elements would change for every webstep, however the Law of the wall was respected through all the internal ballistics simulation.

4.8 Propellant Mass Flow Rate

After the internal ballistics simulation, the propellant mass flow rate trace can be compared with the results found in the literature in order to validate our model. The results are compared with the results of Cavallini [11]:

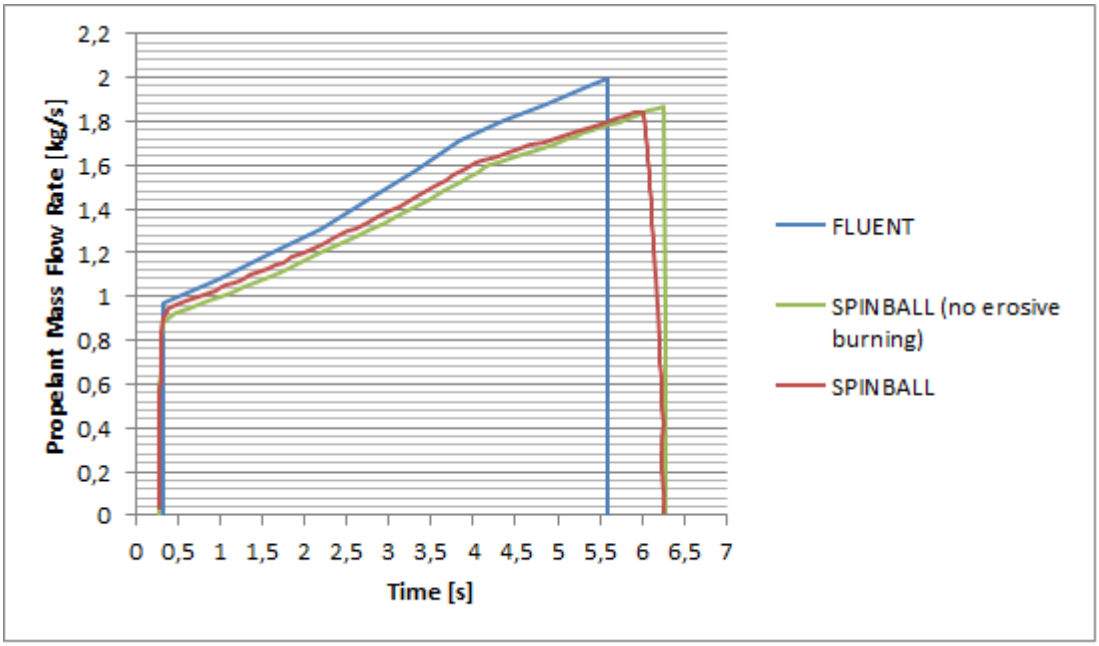

Figure 4.6: Propellant mass flow rate.

We can visualize in the results of our simulation that the propellant burns slightly faster, approximately $0,7\ s$. This difference may be due to the assumption that there is a thin layer of sliver in our model, to the difference in the last webstep as explained previously, and to the combustion parameter assumed.

Furthermore, we can conclude that the results obtained for the propellant mass flow rate are approximate to the values of Cavallini [11]. Thus, we can conclude that the results obtained in the simulation are satisfactory.

4.9 Burning Rate

The results obtained for the burning rate, using Saint Robert's law, can be compared with the results of Cavallini [11], which uses a model that takes into account the contribution of the dynamic burning, with and without the contribution of the erosive burning:

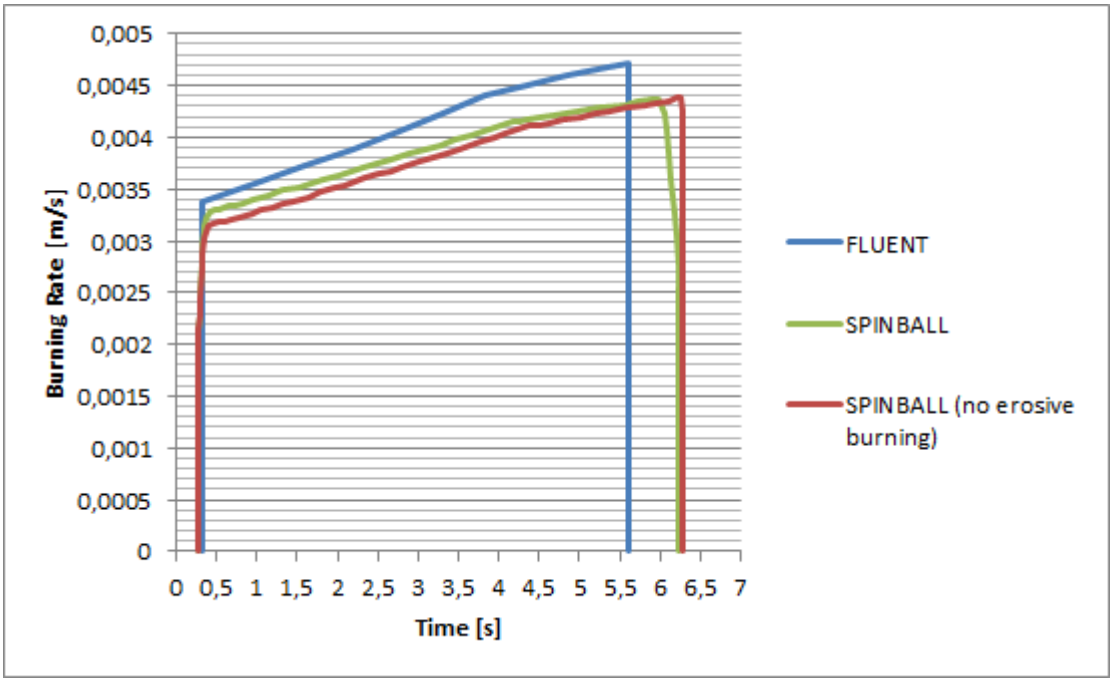

Figure 4.7: Burning rate.

We can conclude that the results obtained for the burning rate are similar to the results of Cavallini [11], although Cavallini uses a model to calculate the burning rate that takes into account the contribution of dynamic burning with and without the contribution of erosive burning, as mentioned previously. However, according to Cavallini [11], the dynamic burning has no effects on the overall burning rate during the QSS. Furthermore, we observe that the contribution of the erosive burning is quite small. Thus, the assumptions that there is no contribution of the dynamic and erosive burning seem reasonable.

The difference in the results may be in the assumptions made. A combustion parameter of 10 $\sqrt{\frac{k^2 \times kmol}{J}}$ was assumed, which may not be the case in the work of Cavallini [11]. Furthermore, we can conclude that the results obtained for our model are satisfactory and even robust.

The results of the burning rate along the motor centerline for time $\approx 5\ s$ can be observed and compared with the results of Wilcox et al. in figure 4.8:

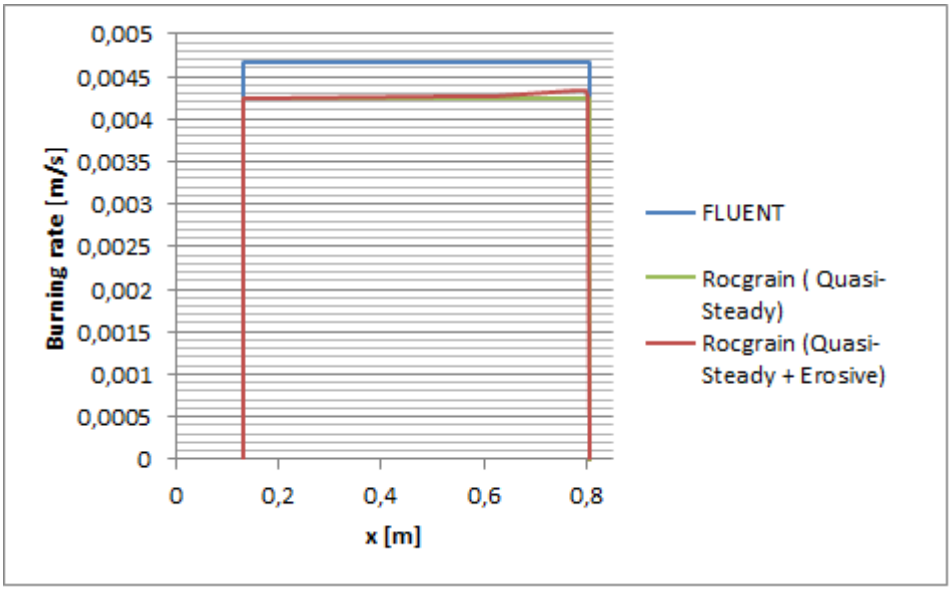

Figure 4.8: time ≈ 5 s.

Analysing the results above, we can see that the results in our internal ballistics simulation are higher than the results of the numerical tool Rocgrain [23]. Furthermore, once more, we can also observe that the contribution of the erosive burning is quite small in the burning rate results. Thus, the assumption that there is no contribution of the erosive burning in our model once again seems to be reasonable.

4.10 Chamber Pressure

The experimental and simulated pressure traces have been compared in order to validate our model. Note that the time has been shifted because the IT phase is not included in the model, as mentioned above. The pressure trace obtained in ANSYS FLUENT, is the mass-average absolute pressure in the chamber trace. The results obtained in our internal ballistics simulation can be compared with the experimental results and the Rocgrain results, with dynamic and quasi-steady burning, from the work of Wilcox et al. [23], as shown in figure 4.9:

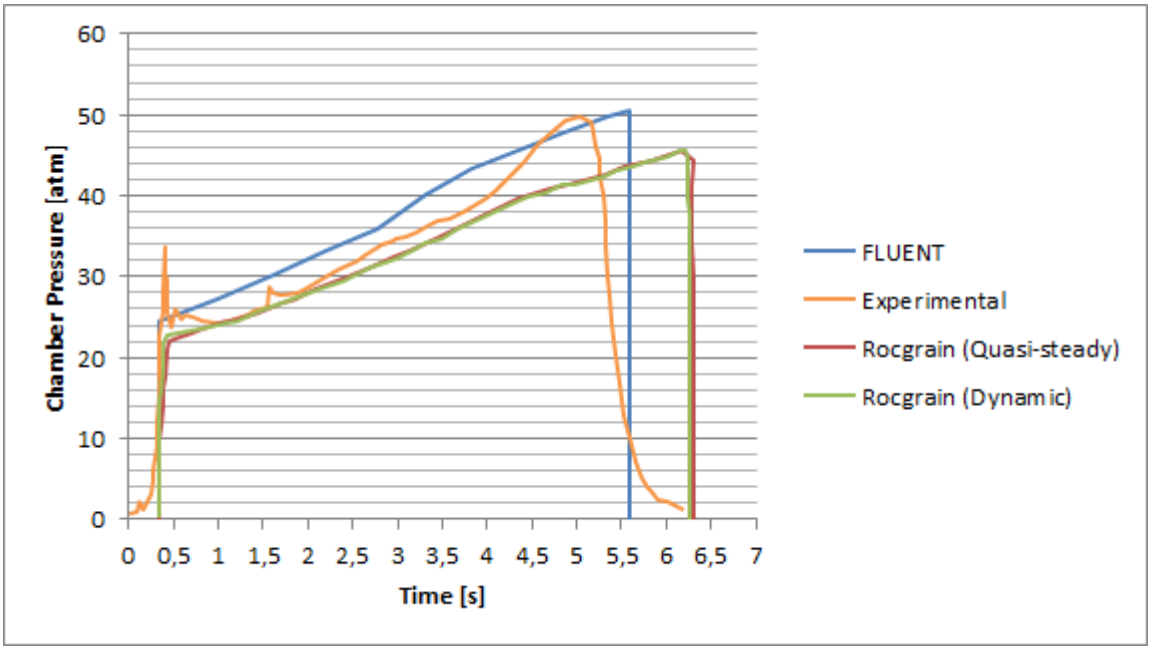

Figure 4.9: Chamber pressure in atm.

Comparing the results, we can conclude that the results obtained in our internal ballistics simulation are satisfactory and robust. We can also assume that the assumptions made are reasonable for this study. As we can observe, the burning time of the propellant is approximately the same in our simulation and in the experimental results.

Although the contribution of the dynamic burning was not simulated in this model, the results of Rocgrain show that the contribution of the dynamic burning in this motor is quite small.

Analysing the Rocgrain results, we observe that the burning time of the propellant is higher than the result of our internal ballistics simulation, which are closer to the experimental results. So now, it is clear why the burning rate in our simulation is higher than the burning rate modelled in Rocgrain. If the propellant has a higher burning rate it means that the burning time of the propellant will be shorter.

The nature of the pressure spike in the experimental trace ($t \approx 0.3\ s$), although not quite clear, is attributed to an ignition phenomena, and/or caused by an erosive burning effect [11]. The phenomenon is related to the combined effects of the igniter jet erosive burning of the grain propellant surface and the igniter tail off, during the end of IT, which is not modelled in this simulation, thus, is not captured in the results of our internal ballistics model.

The last part of the experimental trace, where is seen a pressure rising, suddenly before the TO phase and the consequently the TO phase are not captured and is

quite difficult to explain [11], as in countertrend with the burning surface evolution.

Since there is no effect of the dynamic burning, the slope of the pressure rising is quite well defined, since related only to the progressive behaviour of the grain shape.

Furthermore, we can also compare the results obtained with the results available from the numerical tool (SPINBALL), implemented by Cavallini, with and without the contribution of the erosive burning [11]:

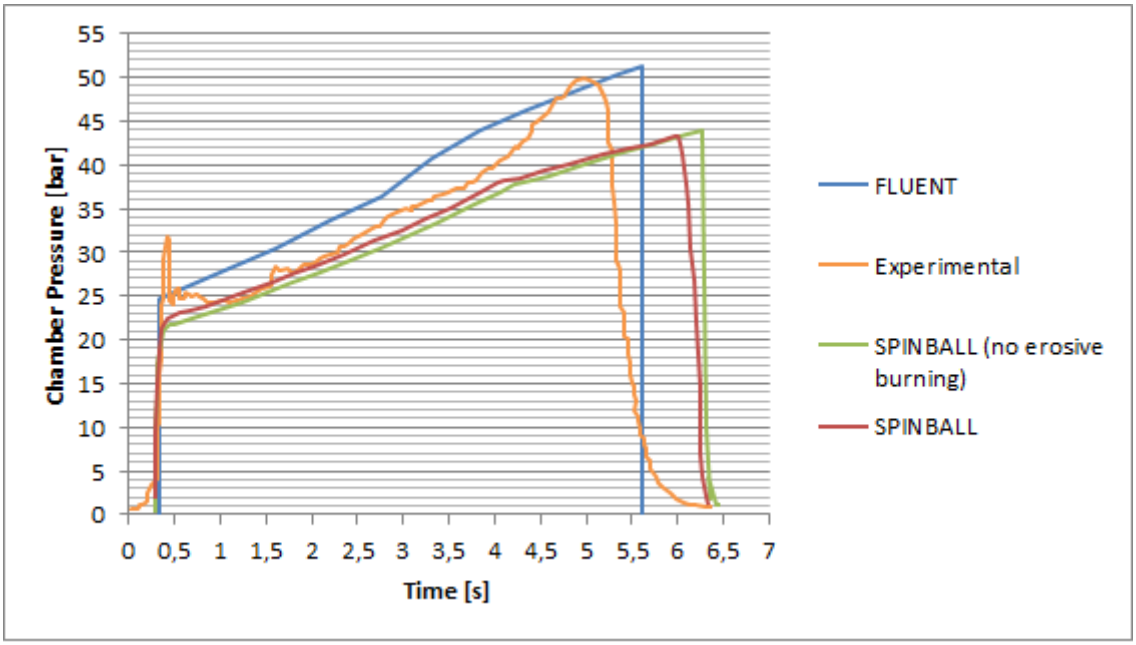

Figure 4.10: Chamber pressure in bar.

Once again, observing the results, we can see the overshoot in the results of our simulation, however, we can conclude that there is an agreement between our results and the experimental results, and even with results of Cavallini [11]. Thus, we can assume that our model is validated by the experimental results and by the multiple numerical tools results, Rocgrain and SPINBALL, available in the literature.

Although the contribution of the erosive burning was not simulated in this model, the results of SPINBALL show, just as shown in section 4.9, that the contribution of the erosive burning in this motor is quite small.

In the work of Wilcox et al., the authors hypothesised that this sudden rise of the pressure in the last part of the QSS phase could be accounted considering the effect of the erosive burning. However, since the SPINBALL results considering the erosive burning contribution does not capture the sudden pressure rise, that hypothesis seems to be excluded. Thus, the nature of the sudden pressure rising

in the last part of the SPRM QSS phase needs to be intensively studied.

The contours obtained with ANSYS FLUENT for the tenth webstep, approximately 5 s, can be seen in figure 4.11:

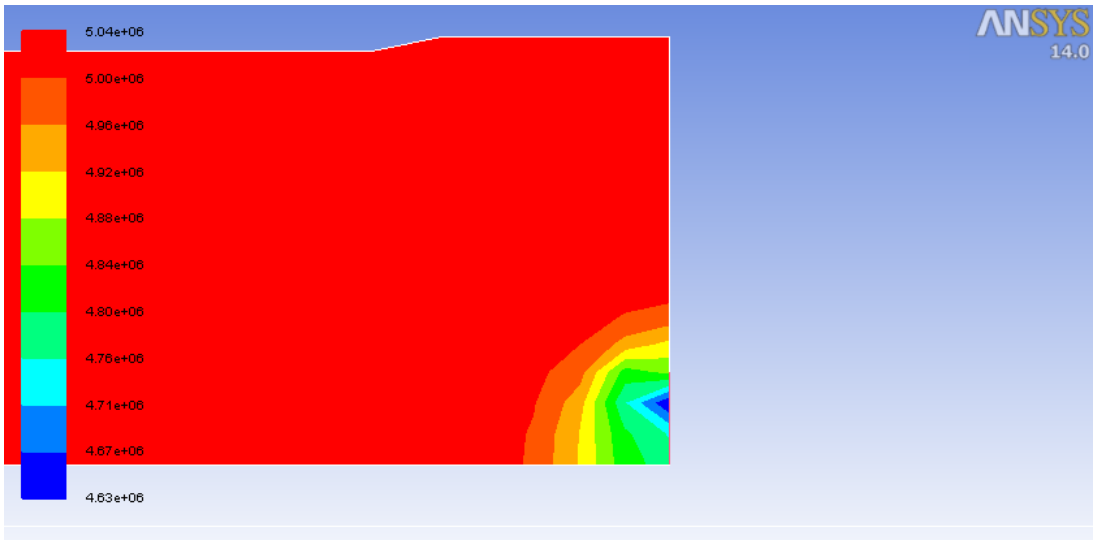

Figure 4.11: Contours of the absolute pressure [Pa] near the throat.

Observing the figure above, we can visualise that the pressure is similar for most of the free volume except for the region near the throat, where it decreases rapidly near the region of the throat.

4.11 Mach Number

The Mach number in the combustion chamber along the centerline obtained from the internal ballistics simulation show a progressive rise in the Mach number followed by a sudden spike near the throat 4.11. The results obtained can also be compared with Cavallini's [11]:

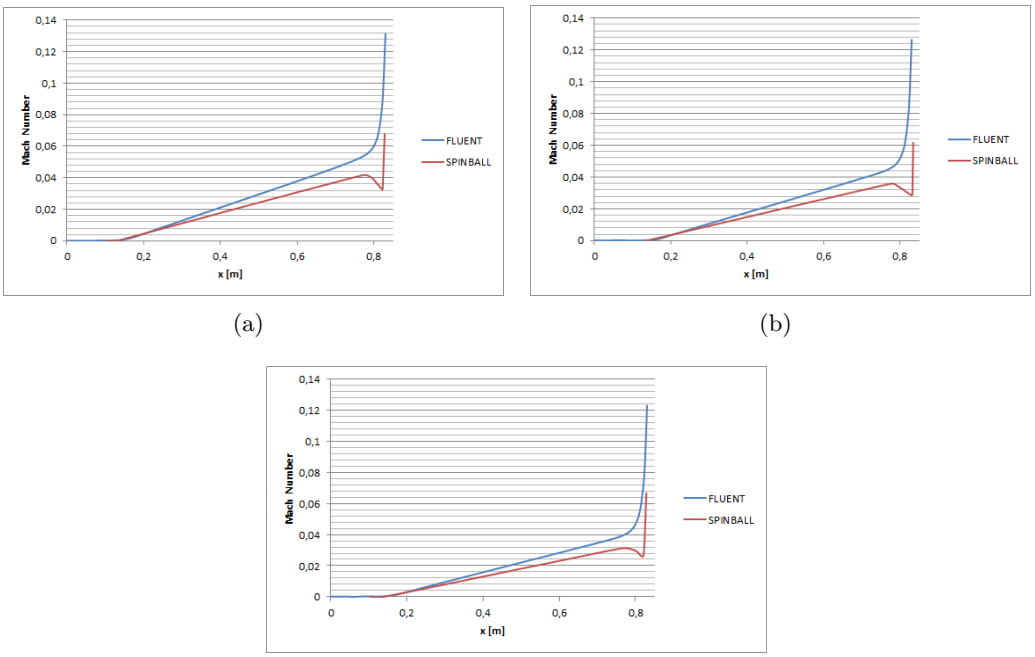

(a) (b)

(c)

Figure 4.12: (a)Time $\approx 3\ s$, (b) Time $\approx 4\ s$, and (c)Time $\approx 5\ s$.

Analysing the results obtained for the Mach number along the centerline from the FLUENT simulation, we can conclude that the results are similar with the results of SPINBALL, although the results of SPINBALL show a decreasing in the Mach number before the sudden spike that is not present in the FLUENT results. Also, we can observe that for the the first $x \approx 0,15\ m$ in the combustion chamber, the Mach number is close to zero.

In figure 4.13 we can observe the results of the numerical simulation for the Mach number in the combustion chamber.

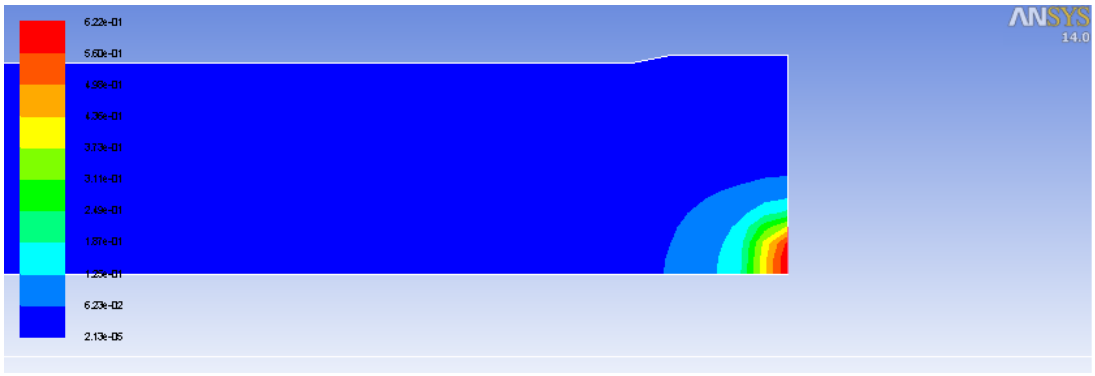

Figure 4.13: Contours of the Mach number near the throat for time $\approx 5\ s$.

Chapter 5

Conclusion

In this study, a 2-D axisymmetric internal ballistics model was developed to simulate the Solid Propellant Rocket Motor internal flowfield conditions during the Quasi Steady State. However, for the motor studied, the NAWC no. 13, the delay in the ignition of the propellant at the aft end compared with that at the end due to flame spreading is insignificant. Thus, the assumption that the whole propellant ignites simultaneously is reasonable.

At the state of the art of the open literature it is, in fact, quite difficult to find SPRM internal ballistics models able to simulate the entire motor combustion time, from the Ignition Transient to Tail Off. Hence, the modelling method in this study simplifies the analysis of the SPRM. Furthermore, no details of the igniter configuration for the NAWC no. 13 are given. Thus, it was not possible to perform a simulation of the IT phase.

The results of the internal ballistics simulation show an agreement with experimental results provided by Wilcox et al. [23] and with the results of other internal ballistics models, Rocgrain, GREG and SPINBALL [23, 11]. This way, validating the internal ballistics model constructed in this study. Therefore, we can conclude that the assumptions made in the construction of the model are reasonable.

Because erosive burning was not simulated in the internal ballistics model, and the results were validated by the experimental traces, we can conclude that the contribution of erosive burning in this motor is small.

The APN model used to calculate the burning rate approximates the burning rate as solely dependent on the mean local pressure using the Vieille's or Saint Robert's law. Thus the contribution of dynamic and erosive burning are not included in the simulation. However, the pressure traces obtained in the internal ballistics simulation are satisfactory and robust. Thus, the selection of the model to calculate the burning rate is reasonable.

The nature of the sudden pressure rising in the last part of the SPRM QSS phase needs to be intensively studied. Perhaps it could be studied with the presented model, however, that goes over the scope of this study.

In conclusion, the internal ballistics model created provides robust and satisfactory results for the SPRM studied. Although not all the phases were included in the model, the IT and TO were not included, the assumptions made in the construction of the model are reasonable and allow us to have satisfactory results without those phases included in the model. Furthermore, the results obtained are validated by experimental results and by the work found in the literature [23, 11], showing that a commercial numerical tool, ANSYS FLUENT, can be used to simulate and predict the behaviour of the given motor in its operative conditions.

Certainly, the next step will be to include other ballistic phenomena not simulated in this model. The SPRM model used in this study is a 2-D axisymmetric model. Typically, grain designs are more complicated, like the example provided in figure 2.13. The use of axial slots, fins, and other possible shapes makes it necessary to model the grain in 3-D space.

Another step could be related to the number of websteps. In fact, the number of websteps could be increased in an automatic manner, i.e, the number of websteps could be increased and the geometry and boundary conditions could be applied automatically by ANSYS FLUENT.

Furthermore, it has been concluded that the contribution of the erosive burning and of the dynamic burning was small in this motor. The same may not happen to other motors. So, another model to calculate the burning rate to capture the erosive burning, or even the dynamic burning may be implemented. The Zel'dovich and Novozhilov method or the Lenoir and Robillard method [23] are highly recommended.

As a final suggestion for future work, the Ignition Transient and Tail Off may be included in the internal ballistics model in order to obtain the pressure spike which nature is due to an ignition phenomena and the tail off phase which is not captured by this model.

References

[1] Hazards of chemical rockets and propellants. Chemical Propulsion Information Agency, May 1972.

[2] *Solid Propellant Grain Design and Internal Ballistics*. NASA, 1972.

[3] L. Caveney A. Peretz, K. Kuo and M. SUmmerfield. Starting transient of solid-propellant rocket motors with high internal gas velocities. *AIAA*, December 1973.

[4] Sevda Aik. Internal ballistic design optimization of a solid rocket motor. Master's thesis, Middle east technical university, May 2010.

[5] Inc. ANSYS. Ansys fluent theory guide. November 2011.

[6] Inc. ANSYS. Ansys fluent user's guide. November 2011.

[7] F. Serraglia B. Favini and M. Di Giacinto. Modeling of flowfield features during ignition of solid rocket motors. 38th AIAA/ASME/SAE/ASEE Joint Propulsion Conference & Exhibit, July 2002.

[8] F. Serraglia B. Favini, S. Zaghi and M. Giacinto. A fully three dimensional analysis of pre-ignition transient in solid rocket motors. 32th AIAA/ASME/SAE/ASEE Joint Propulsion Conference & Exhibit, July 2007.

[9] F. Serraglia B. Favini, S. Zaghi and M. Di Giacinto. 3d numerical simulation of ignition transient induced loads control strategy for vega launcher' solid rocket motors: the zefiro09 static firing test predictions and post firing analysis. 42th AIAA/ASME/SAE/ASEE Joint Propulsion Conference & Exhibit, July 2006.

[10] M. Giacinto B. Favini and A. Neri. Pressuring gas effects on pressure oscilations during the ignition transient of srm. 1st European Conference for AeroSpace Sciences, 2005.

[11] Enrico Cavallini. *Modeling and Numerical Simulation of Solid Rocket Motors Internal Ballistics*. PhD thesis, Sapienza - Universit di Roma, 2009.

[12] F. Dauch and D. Ribereau. A software for srm grain design and internal ballistics evaluation, piball. 38th AIAA/ASME/SAE/ASEE Joint Propulsion Conference & Exhibit, July 2002.

[13] S. Dunn D.coats, J. French and D. Berker. Improvements to the solid performance program (spp). 39th AIAA/ASME/SAE/ASEE Joint Propulsion Conference & Exhibit, July 2003.

[14] Psklc G. Analysis of 3-d grain burnback of solid propellant rocket motors and verification with rocket motor tests. Master's thesis, Dept. of Mechanical Engineering, METU, 2004.

[15] S. Gordon and B. McBride. *Computer Program for Calculation of Complex Chemical Equilibrium Compositions and Applications.* NASA Refence Publication, 1994. Part I.

[16] S. Gordon and B. McBride. *Computer Program for Calculation of Complex Chemical Equilibrium Compositions and Applications.* NASA Refence Publication, 1994. Part II.

[17] T. Crofoot K.Hodge and S. Nelson. Gelled propellants for tactical missile applications. American Institute of Aeronautics and Astronautics, Inc., 1999.

[18] N. Kubota. *Survey of Rocket Propellants and Their Combustion Charateristics.* American institute of aeronautics and astronautics, 1994.

[19] Gore J. Kuo, K. and M. Summerfield. *Erosive Burning of Solid Propellants.* 1984.

[20] Gore J. Kuo, K. and M. Summerfield. *Transient Burning of Solid Propellants.* 1984.

[21] Ilias Lappas. Energy management of advanced rocket systems. Master's thesis, Cranfield university, 2006.

[22] R. Fiedler M. Brandyberry and C. Mclay. Verification and validation of rocstar 3d multi-physics solid rocket motor simulation program. July 2005.

[23] K. Tang M. Wilcox, M. Brewster and D. Steward. Solid rocket motor internal ballistics simulation using three-dimensional grain burnback. *Journal of Propulsion and Power*, 23, 2007.

[24] S. M. Moore. Ballistics modeling of combustion heat loss through chambers and nozzles of solid rocket motors. Master's thesis, B. S., California State University, 2004.

[25] Gordon C. Oates. *Aerothermodynamics of Gas Turbine and Tocket Propulsion*. American Institute of Aeronautics and Astronautics, Inc., third edition, 1997.

[26] W. Flannery F. Boysan D. Choudhury J. Maruzewski S. Orszag, V. Yakhot and B. Patel. Renormalization group modeling and turbulence simulations. International Conference on Near- Wall Turbulent Flows, 1993.

[27] Richard H. Sforzini. An automated approach to design of solid rockets utilizing a special internal ballistics model. June 1980.

[28] George Paul Sutton and Oscar Biblarz. *Rocket Propulsion Elements*. Wiley-Interscience, seventh edition, 2001.

[29] K. Tang and M. Brewster. Dynamic combustion of ap compostite propellants - ignition pressure spike. 37th AIAA/ASME/SAE/ASEE Joint Propulsion Conference and Exhibit, 2001.

[30] P. Thakre and V. Yang. Graphite nozzle material erosion in solip propellant rocket motors. *AIAA*, 2007.

[31] Martin J.L. Turner. *Rocket and Spacecraft Propulsion: Principles, Practice and New Developments*. Praxis publishing, Ltd., third edition, 2009.

[32] R. Fiedler W. Dick, M. Heat and M. Brandyberrry. Advanced simulation of solid propellant rockets from first principles. 41th Joint Propulsion Conference, July 2005.

[33] D. C. Wilcox. *Turbulence Modeling for CFD*. DCW Industries, 1993.

[34] Vuillot F. Yumusak, M. F. and T. Tinaztepe. Viscous internal flow applications for solid propellant rocket motors. *AIAA*, 2006.